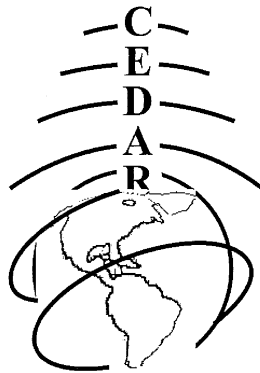


CEDAR

2012

Eldorado Hotel
Santa Fe, New Mexico



IT Poster Session
Tuesday June 26, 2012



Table of Contents

Coupling of the Upper Atmosphere with Lower Altitudes

COUP-01 , Chao-Yen Chen, Seismo-Traveling Ionospheric Disturbances Triggered by the 2011 Tohoku Earthquake Observed by FORMOSAT-3/COSMIC.....	1
COUP-02 , Yosuke Yamazaki, Response of the Ionospheric Current System to Stratospheric Sudden Warmings.....	1
COUP-03 , McArthur Jones, Non-Migrating Tides in the Thermosphere: In-situ Versus Tropospheric Sources.....	1
COUP-04 , Kristi N. Warner, Latent tidal heating variability due to the El Niño—Southern Oscillation.....	2

Data Assimilation

DATA-01 , Sumanta Sarkhel, Penn State Airglow Imagers at Arecibo Observatory: Operation and Image Analyses.....	2
DATA-02 , Robert Sorbello, An Overview of a Cognitive Radar System to Study Plasma Irregularities near the Peruvian Andes	3

Equatorial Ionosphere or Thermosphere

EQIT-01 , Daisuke Fukushima, Geomagnetic conjugate observations of plasma bubbles and thermospheric neutral winds at equatorial latitudes.....	3
EQIT-02 , Henrique Carlotto Aveiro, 3-D numerical simulations of equatorial spread F: results and diagnostics in the Peruvian sector.....	4
EQIT-03 , Carlos Martinis, Conjugate observations of ionospheric processes in the American sector	4
EQIT-04 , Daniel J. Fisher, Comparison of HWM and MSIS and FPI data from Brazil	4
EQIT-05 , Dhvanit Mehta, 24-Hr Thermospheric Winds Measured During the 2011 CORRER Campaigns: Correlation of the pre-reversal enhancement with daytime thermospheric winds.....	5
EQIT-06 , Marc Hairston, Vertical and Meridional Ion Flows Observed by C/NOFS During the 26 September 2011 Storm.....	5
EQIT-07 , Andrew Kiene, Inertial instability analysis of the F-region equatorial neutral zonal jet.....	5
EQIT-08 , Brian D. Tracy, Zonal Plasma Drifts During Extremely Low Solar Flux	6
EQIT-09 , Woo Kyoung Lee, Solar zenith angle effect on the longitudinal plasma distribution in the low-latitude F region	6
EQIT-10 , Roger Hale Varney, Sources of Variability in Equatorial Topside and Plasmaspheric Temperatures.....	6
EQIT-11 , Wu Kang-Hung, Evaluation of Abel inversion error in the different season	7
EQIT-12 , Ryan Davidson, Thermospheric Responses to Geomagnetic Storms	7

EQIT-13 , Paul Zabłowski, Inter-hemispheric and longitudinal studies of ionospheric perturbations from all-sky imagers in the American sector.....	7
EQIT-14 , Esayas B. Shume, Spectral analysis of scintillation measurements at equatorial latitudes	8

Irregularities of the Ionosphere or Atmosphere

IRRI-01 , Esayas B. Shume, Day-time F region echoes observed by the Sao Luis radar	8
IRRI-02 , Haiyang Fu, Modeling of Plasma Irregularities associated with Artificially Created Dusty Plasmas in the Near-Earth Space Environment	8
IRRI-03 , Alireza Samimi, Experimental and analytical considerations of the threshold power for the generation of ion gyro-harmonic structures during radio wave heating near the second electron gyro-harmonic	9
IRRI-04 , Chad A. Madsen, The Farley-Buneman Instability: A Comparison Between the Ionosphere and Solar Chromosphere.....	9
IRRI-05 , Horton Wendell, Transitions in Ionospheric Turbulence from Farley-Buneman to Drift Gradient Regimes.....	9
IRRI-06 , Eugene Dao, Electromagnetic characteristics of equatorial plasma irregularities.....	10
IRRI-07 Kshitija Deshpande, A forward propagation model of GPS scintillations to investigate high latitude ionospheric irregularities.....	10
IRRI-08 , Hyomin Kim, Ionospheric Irregularities at Substorm Onset: Observations of ULF Pulsations and GPS Scintillations	10
IRRI-09 , Pablo M. Reyes, Small period pulsations in the 150-km irregularities.....	11
IRRI-10 , Accel Abarca, Fluid-Kinetic simulation study of the evolution of a penetrating electron beam measured at the top of the ionosphere and its effect on the ISR	11
IRRI-11 , Alvaro John Ribeiro, A survey of plasma irregularities as seen by the mid-latitude Blackstone SuperDARN radar.....	11
IRRI-12 , Sebastien de Larquier, Characterization of quiet-time mid-latitude ionospheric backscatter observed by SuperDARN radars.....	12
IRRI-13 , Ting-han Lin, The relation between neutral wind shear and mechanism of the FAIs	12
IRRI-14 , Kate Despain, Finite Larmor Radius Effects on Ionosphere Interchange Instabilities	12
IRRI-15 , Alireza Mahmoudian, Excitation Threshold of Stimulated Electromagnetic Emissions SEEs Generated at Pump Frequencies Near the third Electron Gyroharmonic	13
IRRI-16 , Hassanali Akbari, Anomalous ISR scatters from the auroral plasma	13

Instruments or Techniques for Ionospheric or Thermospheric Observation

ITIT-01 , Amanda Mills, High Dynamic Range for the Arecibo Observatory's 430 MHz Receiver.....	14
ITIT-02 , Austin Sousa, Mission Objectives of the VLF Wave / Particle Precipitation Mapper (VPM) CubeSat	14
ITIT-03 , Michael J. Nicolls, Global Observations of the ionospheric E region morphology and variability	14

ITIT-04 , Fabiano S. Rodrigues, Interferometric coherent backscatter radar observations of F-region irregularities in the Brazilian sector	15
ITIT-05 , I-Te Lee, Assimilation of FORMOSAT-3/COSMIC electron density profiles into a coupled Thermosphere/Ionosphere model using ensemble Kalman filtering.....	15
ITIT-06 , Ricardo Farino Alonso, Voice and data communication system based on Software-Defined Radio technology to establish VHF radio links via Equatorial Electrojet	16
ITIT-07 , Thomas W. Gehrels, A two-dimensional minimum mean-square error approach to Fabry-Perot interferometer analysis	16
ITIT-08 , Michael Hirsch, Extended duration high-speed auroral tomography system	17
ITIT-09 , Irfan Azeem, Ionospheric Scintillation Monitoring Using GPS based Space Weather Monitor	17
ITIT-10 , Carl Andersen, Ampules: A New Type of Sounding Rocket Payload for the Measurement of Three- Dimensional, Neutral Winds and Gradients in the Lower Thermosphere	18
ITIT-11 , Ewan S. Douglas, Further Comparison of RAIDS observations to radar-fed model of OII 83.4 nm emission	18
ITIT-12 , Tony Mangogna, Helium Resonance Fluorescence LIDAR.....	18
ITIT-13 , Geoff Crowley, Dynamic Ionosphere Cubesat Explorer (DICE): Early Science Instrument Results.....	18
ITIT-14 , Chi-Yen Lin, The effects of 3D error covariance and background model bias for an ionospheric data assimilation model	19
ITIT-15 , Percy Jesus Condor Patilongo, Estimation of Vertical Drifts using Magnetometer Data with Neural Network.....	20
ITIT-16 , Liyuan Mei, Extended SAMI2 Model in a Double Adiabatic form.....	20
ITIT-17 , Marco Antonio Milla, The effects of Coulomb collisions on H ⁺ , He ⁺ , and O ⁺ plasmas for incoherent scatter radar applications at Jicamarca	21
ITIT-18 , Ramin Jafari, Comparison of Time Domain and Frequency Domain Analysis to Estimate Velocity Profile of Field-Aligned Plasma Irregularities	21
ITIT-19 , Juan Miguel Urco, Particle Image Velocimetry (PIV) measurements of the vector velocity of equatorial spread F irregularities over Jicamarca.....	22
ITIT-20 , Alexander Hackett, A 50-MHz Digital Radar System for Ionospheric Studies	22

Long-Term Variations of the Upper Atmosphere

LTRV-01 , Loren Chang, Inter- and Intra-Annual Variability of Tidal Components Observed in FORMOSAT-3/COSMIC TECs, 2007-2011.....	22
LTRV-02 , Ingrid Cnossen, The effects of changes in the Earth's magnetic field on the magnetosphere, ionosphere and thermosphere.....	23
LTRV-03 , Susan M. Nossal, Investigation of Solar Cyclic and Climatic Trends in Upper Atmospheric Hydrogen Distributions	23

Midlatitude Ionosphere or Thermosphere

MDIT-01, Jonathon Nooner, GPS TEC measurements at Clemson, SC, during Solar Minimum.....	24
MDIT-02, Yang-Yi Sun, Ground-based GPS Observation of SED-associated Irregularities Over CONUS	24
MDIT-03, Aron Dodger, Comparing A Simulated Plasmasphere Using Different Driving Electric Field Models With IMAGE EUV Data.....	24
MDIT-04, Yen-Chieh Lin, Model Simulation Of E Region Electron Density and Sporadic E Layers	25
MDIT-05, Dustin Hickey, Inter-hemispheric and latitudinal comparisons of MTM characteristics	25
MDIT-06, Jia-Ting Lin, Atmospheric and ionospheric waves disturbed from the rocket source detected by a Taiwanese GPS array	25
MDIT-07, Timothy M Duly, Investigation of the parallel transport scheme in SAMI2	26
MDIT-08, Levan Lomidze, Modeling of the Weddell Sea Anomaly: Effects of thermospheric wind	26
MDIT-09, Fu-Yuan Chang, Neutral wind effect on mid-latitude summer nighttime anomaly	27
MDIT-10, Samuel Sanders, Simultaneous Fabry-Pérot interferometer observations of thermospheric winds and dynamics at the Pisgah Astronomical Research Institute and at the Millstone Hill Optical Observatory	27
MDIT-11, Eliana Nossa, Analytical solution of the neutral dynamic stability problem to characterize irregularities at midlatitude sporadic E layers.....	27

Polar Aeronomy

POLA-01, Robert Miceli, Comparison of in situ and ground-based measurements during the MICA sounding rocket flight	28
POLA-02, Tapas Bhattacharya, Role of Ionospheric Boundary Conditions on the Evolution of Field-aligned Currents	28
POLA-03, Qian Wu, Millstone Hill and Palmer Station Fabry-Perot interferometer observations	29
POLA-04, Qian Wu, First Daytime Thermospheric Wind observation by HIWIND	29
POLA-05, Stanley Gene Edwin, Simulating magnetosphere-ionosphere coupling in the TIEGCM.....	29
POLA-06, Hanna Dahlgren, Field-aligned motion and morphology of fine scale breakup arcs	30
POLA-07, Ellen D. P. Cousins, An empirical model of large- and small-scale electric fields in Earth's high-latitude ionosphere.....	30
POLA-08, Russell Cosgrove, Empirical models of Poynting flux and kinetic energy flux constructed from FAST data	31
POLA-09, Russell Cosgrove, A new branch of the ionospheric feedback instability: Importance to E region physics	31
POLA-10, Russell Cosgrove, Correlation as a global measure of geomagnetic activity: Phase boundaries and a precedent line of nodes.....	32
POLA-11, Rasoul Kabirzadeh, CHAMP Estimates of Fluctuating Small-Scale Field-Aligned Currents and Their Relation to Flickering Aurora.....	32

POLA-12 , Steven Watchorn, A Proposed Spatial Heterodyne Spectrometer for Measurement of the Proton Aurora at High Latitude	32
POLA-13 , Yanshi Huang, Altitudinal distribution of Joule heating and its influence on the thermosphere	33
POLA-14 , Xianjing Liu, Altitude and latitude variation of Thermosphere Mass Density Response to Geomagnetic Activity in Composition Transition Regions	33
POLA-15 , Callum Anderson, Vertical Winds in the Southern Auroral Thermosphere Observed Concurrently at E- and F-region Altitudes.....	34
POLA-16 , Gareth William Perry, Coincidental measurements of an F-region plasma patch, with optical, incoherent and coherent scatter radar instruments	34
POLA-17 , Victor Pasko, Infrasonic waves generated by supersonic auroral arcs	35
POLA-18 , Evan Thomas, Direct observations of the role of convection electric fields in the formation of a polar tongue of ionization from storm enhanced density	35

Solar Terrestrial Interactions in the Upper Atmosphere

SOLA-01 , Mariangel Fedrizzi, Improving CTIPe neutral density response and recovery during large geomagnetic storms	36
SOLA-02 , Catalin Negrea, On the Validation effort of the Coupled Thermosphere Ionosphere Plasmasphere electrodynamics Model	36
SOLA-03 , Frederick Wilder, Intense dayside Joule heating during the 5 April 2010 geomagnetic storm recovery phase observed by AMIE and AMPERE	37
SOLA-04 , Jie Zhu, The Thermosphere and Ionosphere Reactions to the 15 February 2011 Solar Flare	37
SOLA-05 , Ja Soon Shim, Ionosphere/Thermosphere Model Assessment during the 2006 AGU Storm: TEC, NmF2 and hmF2.....	37
SOLA-06 , Barbara Emery, Climatology Assessment of Ionosphere/Thermosphere Models in Low Solar Flux Conditions for the CCMC CEDAR Challenge	38
SOLA-07 , Cheng Sheng, Height-Integrated Pedersen Conductivity of Ionosphere from COSMIC Observations	38

CEDAR Workshop – IT Poster Session Abstracts Day 1 – Tuesday, June 26, 2012

Coupling of the Upper Atmosphere with Lower Altitudes

COUP-01 Seismo-Traveling Ionospheric Disturbances Triggered by the 2011 Tohoku Earthquake Observed by FORMOSAT-3/COSMIC - by Chao-Yen Chen

Status of First Author: Student IN poster competition, PhD

Authors: C. Y. Chen, L. K. Pei and Tiger J. Y. Liu

Abstract: Seismo-traveling ionospheric disturbances (STIDs), triggered by the 11 March 2011 M9.0 Tohoku earthquake, were simultaneously observed by total electron content (TEC) derived from ground-based receivers of GPS in Taiwan and Japan, as well as ionospheric electron density profiles of FORMOSAT-3/COSMIC (F3/C). It is found that the Abel inversion and the differential process act as the low- and high-pass filters, respectively. The speed and wavelength of the STIDs in the vertical direction probed by radio occultation (RO) are 2000-2200m/s and 60-70km, respectively. This is for the first time that the STIDs in the vertical direction are reported by means of F3/C RO. The vertical wavelengths of the STIDs are further examined by the Hilbert Huang Transform (HHT).

COUP-02 Response of the Ionospheric Current System to Stratospheric Sudden Warmings - by Yosuke Yamazaki

Status of First Author: Non-student

Authors: A. D. Richmond, and K. Yumoto

Abstract: Recently, it has been realized that stratospheric sudden warmings (SSWs) can have a significant impact on ionospheric variability. The SSW is a meteorological event that is characterized by dynamical changes in the middle atmosphere. It is still not fully understood how ionospheric changes are produced during SSWs. We have analyzed ground magnetometer data to examine SSW effects on the electric current system in the dynamo region of the ionosphere (ca 100-150 km). Our results indicate that SSW effects on the ionospheric current system are due to changes in both solar and lunar atmospheric tides.

COUP-03 Non-Migrating Tides in the Thermosphere: In-situ Versus Tropospheric Sources - by McArthur Jones

Status of First Author: Student IN poster competition, PhD

Authors: McArthur Jones Jr.

Department of Aerospace Engineering Sciences, University of Colorado, Boulder, CO, USA
mcarthur.jonesjr@colorado.edu

Jeffrey M. Forbes

Department of Aerospace Engineering Sciences, University of Colorado, Boulder, CO, USA
forbes@colorado.edu

Maura E. Hagan

High Altitude Observatory, National Center for Atmospheric Research, Boulder, CO, USA
hagan@ucar.edu

Astrid Maute

High Altitude Observatory, National Center for Atmospheric Research, Boulder, CO, USA
maute@ucar.edu

Abstract: The importance of non-migrating (i.e., longitude-variable) tides to the dynamics and electrodynamics of the ionosphere-thermosphere system is now widely recognized. In many cases these tides propagate into the thermosphere from sources in the troposphere, but recent data interpretations suggest the existence of non-migrating tides excited in-situ as well. One source of such in-situ generated tides is non-linear tide-tide interactions. Another source not previously studied, and the focus of this investigation, is the generation of non-migrating tides through ion-neutral interactions moderated by the longitude-dependent ionosphere. We report on numerical experiments performed with the National Center for Atmospheric Research (NCAR) Thermosphere-Ionosphere-Mesosphere-Electrodynamics General Circulation Model (TIME-GCM), during both solar minimum ($F10.7 = 75$ solar flux units) and solar maximum ($F10.7 = 200$ solar flux units) conditions, with realistic magnetic field configuration, and an aligned-dipole configuration. We computed difference fields between simulations with a realistic magnetic field and aligned-dipole configurations to quantify the magnitude of the non-migrating tides excited through ion-neutral interactions. It is important to recognize that, in terms of tidal perturbations residing in the upper regions of the thermosphere (200-500 km), this dependence on solar cycle is opposite to that experienced by tides propagating upwards from the troposphere; therefore, the in-situ generated components could dominate some parts of the tidal spectrum at high levels of solar activity. Our computational results are considered in light of observational studies, which suggest that in-situ generated tides must exist in order to reconcile data-model differences.

COUP-04 Latent tidal heating variability due to the El Niño—Southern Oscillation
 - by Kristi N. Warner

Status of First Author: Student IN poster competition

Authors: K. Warner and J. Oberheide
 Department of Physics and Astronomy
 Clemson University
 Clemson, SC 29634

Abstract: This paper presents latent tidal heating variability due to variations in tropospheric deep convection associated with the El Niño - Southern Oscillation (ENSO). Latent tidal heating rates for various nonmigrating tidal components are computed from TRMM satellite data and compared to the Oceanic Niño Index. In particular the easterly diurnal tides of wavenumbers two and three are examined and compared with thermospheric tidal wind variability from TIDI/TIMED. The strongest tidal response occurs during the La Niña phase of ENSO.

Data Assimilation

DATA-01 Penn State Airglow Imagers at Arecibo Observatory: Operation and Image Analyses - by Sumanta Sarkhel

Status of First Author: Non-student

Authors: Sumanta Sarkhel, John D. Mathews, Shikha Raizada, and Craig A. Tepley

Abstract: Airglow imaging observations have been carried out using Penn State allsky and narrow field-of-view imagers located at Arecibo Observatory (AO) over the years. The operation of these User-Owned, Public-Access (UOPA) airglow imagers are controlled automatically using customized data acquisition programs. At present, the allsky imager is operated at 557.7 nm, 630.0 nm, and 777.4 nm wavelengths. The raw data is sent from AO to the Penn State data server dedicated to this and parallel tasks. The processed data products are openly available for all users online (<http://allsky.ee.psu.edu>) in near real-time. The web interface allows users to choose wavelength of interest to view/download movies/keograms at a particular year/month/day. Similar to allsky imager, the narrow field-of-view (~50o) imager is operated automatically at only 630.0 nm wavelength and is aligned looking parallel to geomagnetic field lines. The raw data is also

sent to the Penn State server and analyzed with all data levels also available online to all users at <http://allsky.ee.psu.edu>. We present some sample events from these systems.

DATA-02 An Overview of a Cognitive Radar System to Study Plasma Irregularities near the Peruvian Andes - by Robert Sorbello

Status of First Author: Student IN poster competition, PhD

Authors: Julio Urbina, jvu1@psu.edu, Zach Stephens, zds110@psu.edu

Abstract: We describe the implementation of a VHF coherent imaging radar in Huancayo, near the Peruvian Andes to initiate continuous monitoring of the plasma structuring in the equatorial ionosphere. The new radar system will utilize cognitive sensing techniques and complement the ionospheric observations conducted by the Jicamarca incoherent scatter radar (ISR), located about 170 km to the west of Huancayo along the geomagnetic equator. The main purpose of the new system will be to obtain uninterrupted images of ionospheric structuring and drifts from Huancayo, which are only probed and sampled intermittently from Jicamarca due to the operation costs and scheduling issues of the more powerful incoherent scatter system. It should be noted that the main advantage of operating an incoherent scatter system to measure the state parameters of the ionosphere is lost intermittently (in space and/or time) when thermal equilibrium conditions are violated and the ionosphere becomes unstable and turbulent. Since such 'events' are quite routine near the geomagnetic equator (e.g., equatorial electrojet, 150 km irregularities, equatorial spread F there is much to be gained by maintaining a continuous monitoring of the turbulent structures and studying their onset and evolution vis a vis ISR observations of ionospheric state parameters in time and space surrounding the turbulent structures and layers. The proposed Huancayo station is in effect a 'child' of Jicamarca in the sense that most of the techniques to be used were first developed at Jicamarca e.g., imaging radar interferometry, drift measurements using 150 km echoes, etc. We report current progress of the construction of the system and initial steps for its deployment.

Equatorial Ionosphere or Thermosphere

EQIT-01 Geomagnetic conjugate observations of plasma bubbles and thermospheric neutral winds at equatorial latitudes - by Daisuke Fukushima

Status of First Author: Student IN poster competition, PhD

Authors: Daisuke Fukushima (STEL, Nagoya University), Kazuo Shiokawa (STEL, Nagoya University), Yuichi Otsuka (STEL, Nagoya University), Michi Nishioka (NICT), Minoru Kubota (NICT), Takuya Tsugawa (NICT), Tsutomu Nagatsuma (NICT)

Abstract: Plasma bubbles are plasma-density depletion which is developed by the Rayleigh-Taylor instability on the sunset terminator at equatorial latitudes. They often propagate eastward after the sunset. The eastward propagation of the plasma bubbles is considered to be controlled by background eastward neutral winds in the thermosphere through the F-region dynamo effect. However, it is not clear how the F-region dynamo effect contributes to the propagation of the plasma bubbles, because plasma bubbles and background neutral winds have not been simultaneously observed at geomagnetic conjugate points in the northern and southern hemispheres. In this study, geomagnetic conjugate observations of the plasma bubbles at low latitudes with thermospheric neutral winds were reported.

The plasma bubbles were observed at Kototabang (0.2S, 100.3E, geomagnetic latitude (MLAT): 10.0S), Indonesia and at Chiang Mai (18.8N, 98.9E, MLAT: 8.9N), Thailand, which are geomagnetic conjugate stations, on 5 April, 2011 from 13 to 22 UT (from 20 to 05 LT). These plasma bubbles were observed in the 630-nm airglow images taken by using highly-sensitive all-sky airglow imagers at both stations. They propagated eastward with horizontal velocities of about 100-125 m/s. Background thermospheric neutral winds were also observed at both stations by using two Fabry-Perot interferometers (FPIs). The eastward wind velocities were about 70-130 m/s at Kototabang, and about 50-90 m/s at Chiang Mai. We estimated

ion drift velocities by using neutral winds observed by FPIs and conductivities calculated from the IRI/MSIS models. The estimated velocities were about 10-40 % smaller than the drift velocities of plasma bubbles indicating that 60-90 % of the plasma bubble drift can be explained by the F-region dynamo effect.

EQIT-02 3-D numerical simulations of equatorial spread F: results and diagnostics in the Peruvian sector - by Henrique Carlotto Aveiro

Status of First Author: Student IN poster competition PhD

Authors: Henrique C. Aveiro (hca24@cornell.edu) and David L. Hysell (dlh37@cornell.edu)

Abstract: A three-dimensional initial boundary value simulation of equatorial spread F (ESF) is described. The simulation advances the plasma number density and electrostatic potential forward in time by enforcing the constraints of quasineutrality and momentum conservation. The simulation evolves under realistic background conditions including bottomside plasma shear flow and vertical current. The results are evaluated using three different diagnostics including in situ observations from magnetometers onboard satellites and remote sensing observations made by coherent/incoherent scatter radar and airglow imagers. The diagnostic codes can be used to validate the numerical simulation which is evidently able to reproduce the salient characteristics of ESF observed by these instruments.

EQIT-03 Conjugate observations of ionospheric processes in the American sector - by Carlos Martinis

Status of First Author: Non-student

Authors: J. Baumgardner, C. Brunini, T. Bullett, E. Gularte, D. Janches, M. Mendillo, and P. Zabłowski

Abstract: Optical observations from all-sky imagers at Arecibo, Puerto Rico (18.3° N, 66.7° W, + 28° mag lat) and Mercedes, Argentina (34.6° S, 59.4° W, - 24.5° mag) show simultaneous processes that can be explained only through electrodynamical coupling between both hemispheres. We also present results from ionosonde observations from the USGS San Juan Observatory (18.1° N, 66.15° W) and La Plata (34.9° S, 57.9° W), near the Arecibo and Mercedes Observatories, respectively, as well as TEC and phase fluctuations observations from GPS receivers collocated with the radio and optical instruments. These studies represent the initial attempts toward a comprehensive understanding of thermosphere-ionosphere processes at low-middle latitudes obtained with clusters and networks of instruments that can measure local and magnetically conjugate parameters.

EQIT-04 Comparison of HWM and MSIS and FPI data from Brazil - by Daniel J. Fisher

Status of First Author: Student IN poster competition

Authors: D. J. Fisher - University of Illinois - dfisher2@illinois.edu
J. J. Makela - University of Illinois - jmakela@illinois.edu
J. W. Meriwether - Clemson University - john.meriwether@ces.clemson.edu
R. A. Buriti - Universidade Federal de Campina Grande - rburiti@df.ufcg.edu.br
A. F. Medeiros - Universidade Federal de Campina Grande - afragoso@df.ufcg.edu.br

Abstract: We compare the thermospheric neutral wind climatology from two versions of the Horizontal Wind Model (HWM93, HWM07) as well as the neutral temperature climatology from the Naval Research Lab's Mass Spectrometer and Incoherent Scatter Empirical model (NRLMSISE-00) with Fabry-Perot interferometer (FPI) estimates of these parameters derived from observations of the 630.0-nm emission obtained from northeast Brazil. These models are used extensively in the upper atmosphere community as representations of the baseline neutral state. Although these climatological models are based upon vast

quantities of data, they fail to accurately capture the seasonal patterns and variations of the 250-km region winds and temperatures. A collection of three years of data from Brazil will be presented to show the contrast between the HWM93 and HWM07 climatologies. Comparisons of neutral temperatures highlights the lack of a Midnight Temperature Maximum (MTM) in the NRLMSISE model, although the temperatures compare favorably otherwise.

EQIT-05 24-Hr Thermospheric Winds Measured During the 2011 CORRER Campaigns: Correlation of the pre-reversal enhancement with daytime thermospheric winds - by Dhvanit Mehta

Status of First Author: Student NOT in poster competition, Masters

Authors: Dhvanit Mehta, Andrew J Gerrard, Erick Vidal Safor, John W Meriwether, Erhan Kudeki, Jon Makela, Jorge Chau, Greg Earle

Abstract: In this paper we present both night and day thermospheric wind observations made with the Second-generation, Optimized, Fabry-Perot Doppler Imager (SOFDI), a novel triple-etalon Fabry-Perot interferometer (FPI) designed to make 24-hour measurements of thermospheric winds from OI 630-nm emission. These results were obtained from under the magnetic equator at Huancayo, Peru during the summer 2011 CORRER Campaigns. We report that the thermospheric wind measurements are highly correlated to the strength of the pre-reversal enhancement. This relationship is discussed in light of recent ESF formation theories.

EQIT-06 Vertical and Meridional Ion Flows Observed by C/NOFS During the 26 September 2011 Storm - by Marc Hairston

Status of First Author: Non-student

Authors: Marc Hairston, W. R. Coley, Russell Stoneback, R. A. Heelis (all at University of Texas at Dallas)

Abstract: The magnetic storm that occurred on 26 September 2011 provided an ideal case for investigating the vertical and meridional ion drift response in the equatorial ionosphere. The storm was preceded by five days of extremely quiet conditions (21-25 September 2011), the storm commenced after 15 UT on 26 September, and recovered during the following day (27 September). During this period the perigee (~ 395 km) of the C/NOFS spacecraft was on the dayside between 12 and 13 hours solar local time (SLT). Because of the location of the perigee and the increased ion density in the ionosphere at that time, the CINDI instrument onboard C/NOFS was able to provide reliable ion flow data between 8 and 22 hours SLT allowing us to follow the response of the vertical and meridional flows before, during, and after the storm. We will focus on the surprising lack of upward ion flow enhancements and the predominance of enhanced downward ion flows during the storm.

EQIT-07 Inertial instability analysis of the F-region equatorial neutral zonal jet - by Andrew Kiene

Status of First Author: Student IN poster competition

Authors: A. Kiene and M. F. Larsen
Department of Physics & Astronomy
Clemson University
Clemson, SC, USA

Abstract: Inertial instability in the atmosphere is a fundamental packet type instability in which an imbalance in the horizontal forces leads to amplifying meridional excursions in a zonal flow and the

generation of waves. The instability criterion depends on the sign of the difference between the Coriolis parameter and the meridional gradient of the mean zonal flow. Because of the small value of the Coriolis parameter near the equator, the low-latitude regions are especially susceptible to this type of instability, as has been shown in a number of analyses of equatorial flows at altitudes below the thermosphere. Recent results based on CHAMP satellite data have shown the presence of a zonal jet in the F region that follows the magnetic equator, i.e., a region close to but not generally coincident with the geographic equator. The large winds imply decreasing winds on either side of the maximum and thus significant meridional gradients in the zonal winds, which suggests that the conditions for inertial instability may exist. Here we analyze some of the wind observations to determine the stability of the flow with respect to inertial instability.

EQIT-08 Zonal Plasma Drifts During Extremely Low Solar Flux - by Brian D. Tracy

Status of First Author: Student IN poster competition

Authors: B.D. Tracy¹, B.G. Fejer¹

1. Center for Atmospheric and Space Sciences, Utah State University, Logan Utah, USA

Abstract: We study the seasonal dependence of the equatorial F region zonal electrodynamic plasma drifts using Jicamarca incoherent scatter radar measurements during the 2008-2010 low solar flux period. These data are compared with results from previous low solar flux periods derived from the (Fejer, et. al. 2005) model. We also compare the radar climatology with CNOFS satellite observations and present the initial results from the short term variability (few days) analysis of these drifts.

EQIT-09 Solar zenith angle effect on the longitudinal plasma distribution in the low-latitude F region - by Woo Kyoung Lee

Status of First Author: Non-student

Authors: Woo Kyoung Lee (UCAR/COSMIC project office, wklee@ucar.edu), Hyosub Kil (JHU/APL, Hyosub.Kil@jhuapl.edu), Yong-Sil Kwak (KASI, yskwak@kasi.re.kr)

Abstract: Large-scale longitudinal asymmetry that is represented by a wave number 1 structure exists in the equatorial plasma distribution in the topside. However, our preliminary results obtained from COSMIC data show that the longitudinal asymmetry is variable with altitude. In this study, we investigate the existence of a persistent wave number 1 feature in plasma density by analyzing CHAMP and COSMIC data. Creation of the wave number 1 features is understood in association with the geomagnetic field configuration, but the detailed physical process of the creation of the wave number 1 feature by the geomagnetic field configuration is unknown. We hypothesize that the variation of the solar zenith angle in the magnetic equatorial region plays a significant role in the creation of the wave number 1 feature. We investigate the combined effect of the geomagnetic field configuration and solar zenith angle on the plasma production rate using the Chapman function. By comparing the observation and model calculation results, we validate our hypothesis.

EQIT-10 Sources of Variability in Equatorial Topside and Plasmaspheric Temperatures - by Roger Hale Varney

Status of First Author: Student IN poster competition

Authors: Roger H. Varney, David L. Hysell and Joseph D. Huba

Abstract: Jicamarca measurements of electron temperatures in the topside ionosphere and inner plasmasphere (600-1500 km) from the last solar minimum routinely vary by hundreds of K from day to day despite virtually no variability in the solar flux or geomagnetic activity. Possible sources of these variations are discussed using the SAMI2-PE model, which includes a multi-stream photoelectron transport model.

Changes to the background neutral density and temperature profiles have a modest effect on the high altitude temperatures but not nearly enough to explain the observed variability. The electric fields and thermospheric meridional winds, however, can both substantially change the electron densities and temperatures in the topside ionosphere and inner plasmasphere. The temperatures at these high altitudes are primarily determined by a balance between heating from photoelectrons which travel up the field lines and thermal diffusion which carries heat back down the field lines. The winds and electric fields will change the altitude and densities of the off-equatorial F-regions, especially on the field lines connected to the equatorial anomalies. The densities and temperatures in the plasmasphere will self consistently adjust themselves to be in diffusive equilibrium with the off-equatorial F-regions. Furthermore, decreases in the density and/or altitude of the F-region makes it easier for photoelectrons to escape to high altitudes. These connections between the equatorial plasmasphere, the off-equatorial F-regions, and the neutral thermosphere suggest that future high altitude measurements at Jicamarca could be used to study thermospheric variability.

EQIT-11 Evaluation of Abel inversion error in the different season
- by Wu Kang-Hung

Status of First Author: Student IN poster competition, PhD

Authors: Wu Kang-Hung

Abstract: The errors of the spatial and temporal electron density distributions retrieved by Abel inversion are systematically examined. The electron density profiles are retrieved from the integrated total electron content along the GPS-LEO path simulated by IRI model during March, June, September and December 2008. The IRI electron density profiles are considered as true values and compare with retrieved electron density profile through Abel inversion. Whether day or night, the retrieved electron densities in F2 region are generally coincidence with the true values and the relative errors are below 30%. In contrast to F2 region, the relative error in E and F1 region are larger and approach to 200% in the spring and autumn equinox, but in the summer and winter solstice, it seems to be smaller (below 80%). During nighttime, the retrieved electron densities in the lower ionosphere are totally disordered and false. In the early morning and late afternoon, the EIA effect seem to be not too strong to affect retrieved electron density in the lower ionosphere, and the relative deviation are smaller than in the noon. All the results show the errors are caused by the asymmetric electron density distributions (EIA effect) which violate the assumption of the radio occultation.

EQIT-12 Thermospheric Responses to Geomagnetic Storms - by Ryan Davidson

Status of First Author: Non-student, PhD

Authors: Davidson R. L., Earle G. D., Weimer D. R.

Abstract: The Cross Track Sensor (CTS) aboard the Communication/Navigation Outages Forecast System (C/NOFS) satellite has been in near-continuous operation since July 2011. This instrument provides the arrival angle of the neutral wind vector relative to the ram face of the satellite as well as estimates of neutral density. Preliminary results during three geomagnetic storms are presented. Sudden density increases and equatorward flows accompany the onset of the storm followed by a gradual recovery period, during which conditions return to pre-storm levels.

EQIT-13 Inter-hemispheric and longitudinal studies of ionospheric perturbations from all-sky imagers in the American sector. - by Paul Zabłowski

Status of First Author: Student IN poster competition Undergraduate

Authors: P. Zabłowski, C. Martinis, C. Sullivan, J. Baumgardner, J. Wroten, M. Mendillo

Abstract: All sky imaging data from Arecibo, PR (18.3N, 66.7W, 28N mag lat) and Mercedes, Argentina (34.6S, 59.4W, 24.5S mag. lat.) are used to study 630.0 nm airglow perturbations related to medium-scale traveling ionospheric disturbances (MSTIDs), equatorial spread F (ESF), and brightness waves (BW), the optical signature of the midnight temperature maximum (MTM). The Mercedes all-sky imager is very close to the geomagnetic conjugate point of Arecibo. This allows for direct inter-hemispheric imaging of conjugate processes during the period 2009-2011. In addition, another imager located at El Leoncito, Argentina (31.8S, 69.3W, 18S mag. lat.) is used to study the longitudinal dependence of these processes in the southern hemisphere.

EQIT-14 Spectral analysis of scintillation measurements at equatorial latitudes
- by Esayas B. Shume

Status of First Author: Non-student

Authors: Esayas Shume, JPL, Pasadena, CA; Tony Mannucci, JPL, Pasadena, CA; Xiaoqing Pi, JPL, Pasadena, CA; Mark Butala, JPL, Pasadena, CA

Abstract: The poster will present spectral analysis of GPS scintillation measurements in the South American equatorial region. Implication of the spectral analysis for scintillation forecasting and development of large scale plasma irregularities will also be addressed.

Irregularities of the Ionosphere or Atmosphere

IRRI-01 Day-time F region echoes observed by the Sao Luis radar
- by Esayas B. Shume

Status of First Author: Non-student

Authors: Esayas Shume, JPL; Fabiano Rodrigues, UT Dallas; Eurico de Paula, INPE; Inez Batista, INPE; David Galvan, JPL

Abstract: The poster presents unique day-time F region coherent scatter echoes observed by the 30 MHz radar in Sao Luis, Brazil. Simultaneous GPS TEC and ionosonde measurements from Sao Luis will also be presented.

IRRI-02 Modeling of Plasma Irregularities associated with Artificially Created Dusty Plasmas in the Near-Earth Space Environment - by Haiyang Fu

Status of First Author: Student IN poster competition

Authors: Haiyang Fu, Wayne Scales
Bradley Department of Electrical and Computer Engineering, Virginia Tech, Blacksburg, VA, USA
haiyangf@vt.edu
wscales@vt.edu

Abstract: Plasma turbulence associated with the creation of an artificial dust layer in the earth's ionosphere is investigated. The Charged Aerosol Release Experiment (CARE) aims to understand the mechanisms for enhanced radar backscatter from plasma irregularities embedded in dusty plasmas in space. The plasma irregularities embedded in artificial dusty plasma in space may shed light on understanding the mechanism for enhanced radar scatter in the natural dust layers in the earth's mesosphere (NLCs and PMSEs) and also contribute to addressing possible effects of combustion products in rocket and shuttle exhaust in the upper atmosphere as well.

A variety of plasma irregularities can be generated in such active experiments. Computational models are described to study plasma irregularities in artificially created dusty space plasmas, which may lead to radar

echoes. Possible irregularities, in the magnetized dusty plasma, are the shear-driven and streaming instability near the lower hybrid frequency generated by dust streaming perpendicular to the background geomagnetic field. The magnetic field effect on such lower hybrid instabilities are investigated by a model including the ratio of electron plasma frequency and electron gyro frequency. Electrostatic ion cyclotron instability, which may be weak compared to lower hybrid instability, will also be studied by a computational model with electron Landau damping. The dust acoustic (DA) instability and ion acoustic (IA) instabilities in unmagnetized plasmas are also investigated by a model using a Boltzmann electron assumption. Such acoustic type instabilities may be due to the dust and ion streaming along the geomagnetic field. The frequency range and wavelength in a nonlinear saturated state are also estimated for applications to active sounding rocket experiments. These computational models have the advantage of following nonlinear wave-particle effects, which may help designing future experiment.

IRRI-03 Experimental and analytical considerations of the threshold power for the generation of ion gyro-harmonic structures during radio wave heating near the second electron gyro-harmonic. - by Alireza Samimi

Status of First Author: Student IN poster competition, PhD

Authors: Alireza Samimi (arsamimi@vt.edu), Wayne Scales, and Paul Bernhardt

Abstract: Recent experimental observations of the SEE spectrum show structures ordered by ion gyro-harmonic frequencies. The threshold transmitter power required for the excitation of these structures was measured at HAARP facility Gakona, AK. The results indicate that ion gyro-harmonic structures can be generated by a transmitter power as low as 0.4 MW. These experimental observations are in line with the theoretical predictions for the generation mechanism in the upper hybrid altitude.

In this presentation, new experimental observations are presented. Furthermore, theoretical considerations of the electric field strength in the interaction region, threshold level for the parametric decay instability and the oscillating two stream instability are also provided.

IRRI-04 The Farley-Buneman Instability: A Comparison Between the Ionosphere and Solar Chromosphere - by Chad A. Madsen

Status of First Author: Student IN poster competition, Masters

Authors: Chad A. Madsen, Yakov S. Dimant, Meers M. Oppenheim
 Center for Space Physics, Boston University, Boston, MA
 Juan M. Fontenla
 Laboratory for Atmospheric and Space Physics, University of Colorado at Boulder, Boulder, Colorado

Abstract: Strong currents drive the Farley-Buneman instability in the E-region ionosphere creating turbulence and heating. The solar chromosphere is a similar weakly ionized region with strong local Pedersen currents, and the Farley-Buneman instability may play a role in sustaining the thin layer of enhanced temperature observed there. The plasma of the solar chromosphere requires a new theory of the Farley-Buneman instability accounting for the presence of multiple ion species. This work compares this multi-species Farley-Buneman instability to that found in the E-region ionosphere. The multi-species dispersion relation is derived and used to determine the critical electron drift velocity for triggering the instability. Further investigation shows that neutral flows and turbulence in the chromosphere are likely to provide sufficiently large electron drift velocities to trigger the instability.

IRRI-05 Transitions in Ionospheric Turbulence from Farley-Buneman to Drift Gradient Regimes - by Horton Wendell

Status of First Author: Non-student, PhD

Authors: W. Horton, E. Hassan, S. Litt and A. Smolyakov

Abstract: A unified set of nonlinear partial differential equations for the Farley-Buneman and Drift-Gradient ionospheric turbulence are derived and solved numerically. The nonlinear stage in the of the rising plumes and falling higher electron density layer. The presence of the smaller scale turbulent ion acoustic turbulence is associated with strong storms and substorms driven by the solar wind.

IRRI-06 Electromagnetic characteristics of equatorial plasma irregularities
- by Eugene Dao

Status of First Author: Student IN poster competition

Authors: Eugene Dao, Charlie Seyler and Mike Kelley

Abstract: Results from a newly developed 3 Dimensional ElectroMagnetic Model (3DEMM) show the electromagnetic characteristics (both electrostatic and dynamic) of equatorial plasma irregularities.

IRRI-07 A forward propagation model of GPS scintillations to investigate high latitude ionospheric irregularities - by Kshitija Deshpande

Status of First Author: Student IN poster competition, PhD

Authors: Kshitija Deshpande (Virginia Tech), Gary Bust (ASTRA), C. Robert Clauer (Virginia Tech)

Abstract: Study of ionospheric scintillations of radio signal involves the problem of electromagnetic (EM) wave propagation in random media. Modeling GPS scintillations from high latitude ionospheric irregularities can thus be considered as a three dimensional (3D) EM wave forward propagation problem. Additionally, the path of signal from satellite to ground has a variable angle of incidence. This delivers more challenges for the problem in addition to those created by inhomogeneity in the random media of irregularities as well as by the geometry of magnetic field lines at high latitude regions. We have recently developed a full 3D model for EM propagation through random media that is applicable at high latitudes. In this work, we present the recent developments in the model such as addition of high latitude spectrum of irregularities and adding drift velocities to the irregularities. We also attempt to determine sensitivity of the model to different spectral and propagation parameters. Our goal is to utilize this model to solve an inverse problem for a high latitude GPS scintillation observation and understand the turbulence that caused the GPS scintillation. As an initial step towards our goal, we compare results from our model and GPS scintillation data from 24 January 2012 storm from CASES GPS receiver on an AAL-PIP station at the South Pole. With work continued in the same direction, we expect to utilize GPS scintillation measurements in conjunction with ancillary observations from other instruments combined with physical parameters derived from the forward propagation model, and inverse methods to achieve an improved understanding of the physics of the high latitude irregularities.

IRRI-08 Ionospheric Irregularities at Substorm Onset: Observations of ULF Pulsations and GPS Scintillations - by Hyomin Kim

Status of First Author: Student NOT in poster competition

Authors: H. Kim, K. Deshpande, C. R. Clauer (Virginia Tech), M. R. Lessard (University of New Hampshire), A. T. Weatherwax (Sienna College), G. Bust and G. Crowley (ASTRA)

Abstract: While low-latitude ionospheric plasma irregularities, which causes scintillations in GPS signals, have been widely studied, information on high-latitude irregularities are largely unexplored. High latitude ionospheric plasmas, more closely connected to solar wind and magnetospheric dynamics, produce very dynamic and short-lived GPS scintillations making it challenging to characterize them. In this study, the first simultaneous observations of ULF pulsations (Pi2 and Pi1B) and GPS phase scintillations at substorm

onset are presented using a newly designed autonomous, adaptive low-power instrument platform (AAL-PIP) installed at South Pole Station. Both the magnetic field and GPS data appear to be well-correlated in terms of their onset times and spectral structures. Data from Imaging riometer at South Pole Station are also utilized to be compared with the AAL-PIP data. The point of this paper is to address a fundamental question as to whether geomagnetic pulsations associated with enhancements of the auroral currents can generate plasma instability and thus electron density fluctuations observed in GPS signals passing through the disturbed ionosphere.

IRRI-09 Small period pulsations in the 150-km irregularities - by Pablo M. Reyes

Status of First Author: Student NOT in poster competition, Masters

Authors: Reyes, Pablo and Kudeki, Erhan
University of Illinois at Urbana-Champaign

Abstract: The performance of high spatial and temporal resolution observations of 150-km irregularities during the MST-ISR campaigns, show the existence of pulsations with periods on the order of 18 seconds. Kudeki and Fawcett (1993) reported temporal modulation of echo intensities with characteristic periods of approximately 5-15 minutes. In this work we report on backscatter intensity pulsations with periods on the order of a third of a minute.

**IRRI-10 Fluid-Kinetic simulation study of the evolution of a penetrating electron beam measured at the top of the ionosphere and its effect on the ISR
- by Accel Abarca**

Status of First Author: Non-student

Authors: A. Abarca (University of Chile), M. Zettergren (Embry-Riddle Aeronautical University), K. A. Lynch (Dartmouth College), M. A. Diaz (University of Chile), J. L. Semeter (Boston University) and M. Oppenheim (Boston University)

Abstract: A penetrating electron beam measured during the SERSIO campaign at the top of the ionosphere is evolved by using TRANSCAR to obtain the change in the velocity distribution at different altitudes. The velocity distribution at 183 km is used as starting point of an Electrostatic Particle-In-Cell (EPIC) code where the impact of the beam on the ISR spectrum is analyzed. Simulations show that at this altitude, Natural Enhanced Ion Acoustic Waves are developed nearby 500 MHz, the ESR operational frequency, which agrees with ESR observations during the SERSIO campaign.

IRRI-11 A survey of plasma irregularities as seen by the mid-latitude Blackstone SuperDARN radar - by Alvaro John Ribeiro

Status of First Author: Student IN poster competition, PhD

Authors: A. J. Ribeiro, J. M. Ruohoniemi, J. B. H. Baker, L. B. N. Clausen, R. A. Greenwald, M. Lester

Abstract: The Super Dual Auroral Radar Network is a chain of HF radars that monitor plasma dynamics in the ionosphere. In recent years, SuperDARN has expanded to mid-latitudes in order to provide enhanced coverage during geomagnetically active periods. A new type of backscatter from F region plasma irregularities with low Doppler velocity has been frequently observed on the nightside during quiescent conditions. Using three years of data from the Blackstone, VA radar, we have implemented a method for extracting this new type of backscatter from routine observations. We have statistically characterized the occurrence properties of the Sub Auroral Ionospheric Scatter (SAIS) events, including the latitudinal relationships to the equatorward edge of the auroral oval and the ionospheric projection of the plasmapause. We find that the backscatter is confined to local night, occurs on ~70% of nights, is fixed in geomagnetic latitude, and is equatorward of both the auroral region and the plasmapause boundary. We conclude that

SAIS irregularities are observed within a range of latitudes that is conjugate to the inner magnetosphere (plasmasphere).

**IRRI-12 Characterization of quiet-time mid-latitude ionospheric backscatter
observed by SuperDARN radars - by Sebastien de Larquier**

Status of First Author: Student NOT in poster competition, PhD

Authors: S. de Larquier, J.M. Ruohoniemi, J.B.H. Baker, P. Ponomarenko, A.J. Ribeiro

Abstract: The mid-latitude SuperDARN radars regularly observe low-velocity ionospheric backscatter under quiet geomagnetic conditions. Previous work has shown that this type of scatter is confined to local night, occurs on ~70% of nights and lacks significant seasonal variations, and is subauroral and equatorward of the plasmopause boundary. To better understand the irregularities responsible for mid-latitude quiet-time nightside ionospheric backscatter, it is necessary to obtain an accurate description of their spatial extent and drift velocities. We compare range, azimuth and elevation data from the Blackstone SuperDARN radar with modeling results from ray tracing coupled with IRI-2011. The availability of elevation data from the Blackstone radar between 02/2010 and 06/2011 makes possible better evaluation of backscatter altitude and ground range. We are able to account for observation characteristics on the basis of this modeling. We find that the spatial limits of ionospheric backscatter in range and azimuth are generally set by propagation conditions; we infer that the irregularities are widely distributed in the mid-latitude regions. We determine that the ionospheric backscatter occurs at heights of 200-350 km, confirming previous assumptions that the irregularities are located in the F-region. From overall agreement with ray tracing results, we obtain estimates of the correction to apply to the measured velocities to obtain the line-of-sight component of the irregularity drift. We show that this correction is typically very small (~5%). We argue that the ability to closely reproduce observations with propagation modeling yields much greater precision in echo-location, both horizontally and vertically, as well as improved estimation of irregularity drift velocity.

**IRRI-13 The relation between neutral wind shear and mechanism of the FAIs
- by Ting-han Lin**

Status of First Author: Student NOT in poster competition, PhD

Authors: Ting-han Lin

Abstract:

**IRRI-14 Finite Larmor Radius Effects on Ionosphere Interchange Instabilities
- by Kate Despain**

Status of First Author: Non-student

Authors: J.D. Huba, Naval Research Laboratory, Washington, DC

Abstract: Ionospheric irregularities responsible for the scintillation of radiowaves and radar backscatter have scale lengths in the range of 10s - 100s m. At these scales, finite Larmor radius (FLR) effects can become important and affect the evolution of ionospheric instabilities. We have developed a new model to capture FLR effects on ionospheric turbulence and will present nonlinear simulation results to highlight these effects.

**IRRI-15 Excitation Threshold of Stimulated Electromagnetic Emissions SEEs
Generated at Pump Frequencies Near the third Electron Gyroharmonic
- by Alireza Mahmoudian**

Status of First Author: Student NOT in poster competition

Authors: Alireza Mahmoudian

Abstract: The High-Frequency Active Auroral Research Program (HAARP) in Gakona, Alaska provides effective radiated powers in the megawatt range that have allowed researchers to study many non-linear effects of wave-plasma interactions. Stimulated Electromagnetic Emission (SEE) is of interest to the ionospheric community for its diagnostic purposes. In recent HAARP heating experiments, it has been shown that during the Magnetized Stimulated Brillouin Scattering MSBS instability, the pumped electromagnetic wave may decay into an electromagnetic wave and a low frequency electrostatic wave (either ion acoustic IA wave or electrostatic ion cyclotron EIC wave). According to the matching conditions, the O-mode electromagnetic wave can excite either an ion-acoustic wave with a frequency less than the ion cyclotron frequency that propagates along the magnetic field or an electrostatic ion cyclotron (EIC) wave with frequency just above the ion cyclotron frequency that propagates at an angle with respect to the magnetic field. Using Stimulated Electromagnetic Emission (SEE) spectral features, side bands which extend above and below the pump frequency can yield significant diagnostics for the modified ionosphere. It has been shown that the IA wave frequency offsets can be used to measure electron temperature in the heated ionosphere and EIC wave offsets can be used as a sensitive method to determine the ion species by measuring ion mass using the ion gyro-frequency offset.

In this presentation the results of SEE experiment at 2010 PARS summer school and 2011 SSRC will be discussed. The experiment was performed at the 3rd electron gyro harmonic with frequency sweeping, power stepping and beam angle variation. Three diagnostics were implemented to study the SEE. There were 1) A 4 channel spectrum analyzer SEE receiver, 2) the University of Alaska SuperDARN radar facility and, 3) the MUIR incoherent scatter radar.

The experimental results aimed to show the threshold for transmitter power to excite IA wave propagating along the magnetic field line as well as for EIC wave while transmitter antenna beam pointed at an angle with respect to magnetic field.

A full wave solution has been used to estimate the amplitude of the electric field at interaction altitude. This electric field amplitude will be used to estimate the growth rate of IA and EIC waves using the solution of the nonlinear dispersion relation. The estimated growth rate using the theoretical model will be used to make quantitative comparisons with the threshold of SBS lines in the experiment.

IRRI-16 Anomalous ISR scatters from the auroral plasma - by Hassanali Akbari

Status of First Author: Student IN poster competition, PhD

Authors: Hassanali Akbari, hakbari@bu.edu and Joshua Semeter, jls@bu.edu

Abstract: Experimental data obtained with the 449-MHz Poker Flat Incoherent Scatter Radar (PFISR) occasionally shows anomalous scatters at, or close to, the F-region peak. The scatters have common features that distinguish them from the classic Naturally Enhanced Ion Acoustic Lines (NEIALs). The features are (1) greatly enhanced, flat, ion acoustic spectrum (believed to indicate the presence of an additional peak at zero Doppler), and (2) symmetric or asymmetric double-peaked plasma line spectrum. Similar spectral morphologies are observed during active HF ionospheric modification experiments and are considered unmistakable indications of Strong Langmuir Turbulence (SLT).

Instruments or Techniques for Ionospheric or Thermospheric Observation

ITIT-01 High Dynamic Range for the Arecibo Observatory's 430 MHz Receiver - by Amanda Mills

Status of First Author: Student IN poster competition, Masters

Authors: Amanda Mills (acm210@psu.edu) – Pennsylvania State University, Julio V. Urbina (jvu1@psu.edu) – Pennsylvania State University, Ganesan Rajagopalan (ganesh@naic.edu) – Arecibo Observatory, Sixto Gonzales (sixto@naic.edu) – Arecibo Observatory, Mark Wharton (MarkWharton@engr.psu.edu) – Pennsylvania State University

Abstract: This project focuses on improving the dynamic range of the Arecibo Observatory's 430 MHz receiver. The first portion of the project involves designing and testing a high dynamic range low noise amplifier (LNA). The goal is to produce a prototype that will improve the gain and noise figure of the current 430 MHz receiver and also perform well in cryogenic temperatures. The proposed LNA design will also increase the receiver's recovery time from the radar's transmit pulse. The design centers around GaAs high electron mobility transistors (HEMT) selected for low noise characteristics and good performance. The project includes simulations in Agilent Technologies' Advance Design Systems software, schematic/layout design, and prototype testing in room and cryogenic temperatures. The testing phase will require specific techniques to make precise noise temperature measurements in the cryogenic environment. Accurate noise temperature measurements are critical to the development and verification of HEMT cryogenically cooled amplifiers. These measurements shall be made by inserting a cryogenic attenuator at the input of the device under test, a technique common in the field of radio astronomy. When both attenuator and LNA are cooled to cryogenic temperatures, many errors present in the standard cryogenic measurement methods are greatly reduced.

ITIT-02 Mission Objectives of the VLF Wave / Particle Precipitation Mapper (VPM) CubeSat - by Austin Sousa

Status of First Author: Student NOT in poster competition

Authors: Austin Sousa

Abstract: The Earth's radiation belts are comprised of charged particles, which become trapped depending on the particle's parallel and perpendicular kinetic energies. The angle between a particle's parallel and perpendicular velocities is known as a pitch angle. Whistler-mode electromagnetic waves propagating in the magnetosphere have been shown to sufficiently alter a particle's pitch angle, and allow trapped particle populations to precipitate into the ionosphere. The Stanford Very Low Frequency (VLF) group, in partnership with Lockheed Martin, has recently begun designing a nanosatellite, which will provide the first in-situ measurement of wave-induced pitch-angle scattering. Design of the sensor suite will be completed in late 2013, with an expected launch date in 2015.

ITIT-03 Global observations of the ionospheric E region morphology and variability - by Michael J. Nicolls

Status of First Author: Non-student

Authors: M. J. Nicolls, SLAC, Menlo Park, CA
F. S. Rodrigues, The University of Texas at Dallas, Richardson, TX
G. Bust, ASTRA, Boulder, CO

Abstract: The global morphology and variability of the ionospheric E region are estimated from satellite-based radio occultation total electron content (ROTEC) observations. Vertical profiles of E region electron density are estimated using the inversion technique recently proposed by Nicolls et al. (2009). In this technique, the F-region contribution to each ROTEC measurement is removed using an assimilative model

of the ionosphere in order to mitigate the effects of F-region gradients in the estimation of E region profiles. The technique is applied to occultation observations made by GPS receivers onboard COSMIC satellites aided by F-region electron density specification provided by the Ionospheric Data Assimilation Four-Dimensional (IDA4D) algorithm. Global estimates of hmE, NmE, and E region total electron content (TEC) are presented for two different months: April 2007 and January 2008. Results of our analysis show that ROTEC measurements such as those provided by the COSMIC constellation can produce reasonable and valuable estimates of E region parameters on a global scale when properly treated for the effect of F-region density gradients. The agreement between the α -Chapman theory of ionization and recombination and estimated profiles is demonstrated. Reasonable estimates of E region variability can also be specified by the global measurements.

ITIT-04 Interferometric coherent backscatter radar observations of F-region irregularities in the Brazilian sector - by Fabiano S. Rodrigues

Status of First Author: Non-student

Authors: F. S. Rodrigues, The University of Texas at Dallas, Richardson, TX
E. R. de Paula, INPE, Brazil

Abstract: Recent advances in the data acquisition system of the Sao Luis coherent scatter radar interferometer have allowed us to make more continuous observations than previously possible. This upgrade has also allowed us to make observations of ionospheric irregularities for several consecutive hours, which was not possible until recently. Here, we present results of interferometric radar observations made over more than a year (Aug. 2010- Feb. 2012) of F-region irregularities in the Brazilian longitude sector. Results include variability on the morphology of pre-midnight F-region echoes in short time scales (day-to-day), and as a function of season and solar flux conditions. We also present results of the variability in the zonal and vertical velocity of the observed F-region irregularities.

ITIT-05 Assimilation of FORMOSAT-3/COSMIC electron density profiles into a coupled Thermosphere/Ionosphere model using ensemble Kalman filtering - by I-Te Lee

Status of First Author: Student IN poster competition, PhD

Authors: I-Te Lee

Institute of Space Science, National Central University, Chung-Li, 32001, Taiwan

High Altitude Observatory, National Center for Atmospheric Research, Boulder, CO, 80301, USA

Tomoko Matsuo

Cooperative Institute for Research in Environmental Sciences, University of Colorado at Boulder, Boulder, CO, 80309, USA

Space Weather Prediction Center, National Oceanic and Atmospheric Administration, Boulder, Colorado, USA

A. D. Richmond

High Altitude Observatory, National Center for Atmospheric Research, Boulder, CO, 80301, USA

J. Y. Liu

Institute of Space Science, National Central University, Chung-Li, 32001, Taiwan

National Space Organization, Hsinchu 30078, Taiwan

W. Wang

High Altitude Observatory, National Center for Atmospheric Research, Boulder, CO, 80301, USA

C. H. Lin

Department of Earth Science, National Cheng Kung University, Tainan, 70101, Taiwan

J. L. Anderson

Institute for Mathematics Applied to Geosciences, National Center for Atmospheric Research, Boulder, CO, 80305, USA

M. Q. Chen

Abstract: This paper presents our effort to assimilate FORMOSAT-3/COSMIC (F3/C) GPS Occultation Experiment (GOX) observations into the National Center for Atmospheric Research (NCAR) Thermosphere Ionosphere Electrodynamics General Circulation Model (TIE-GCM) by means of ensemble Kalman filtering (EnKF). The F3/C electron density profiles (EDPs) uniformly distributed around the globe provide an excellent opportunity to monitor the ionospheric electron density structure. The NCAR TIE-GCM simulates the Earth's thermosphere and ionosphere by using self-consistent solutions for the coupled nonlinear equations of hydrodynamics, neutral and ion chemistry, and electrodynamics. The F3/C EDP are combined with the TIE-GCM simulations by EnKF algorithms implemented in the NCAR Data Assimilation Research Testbed (DART) open-source community facility to compute the expected value of electron density, which is 'the best' estimate of the current ionospheric state. Assimilation analyses obtained with real F3/C electron density profiles are compared with independent ground-based observations as well as the F3/C profiles themselves. The comparison shows the improvement of the primary ionospheric parameters such as NmF2 and hmF2. Nevertheless some unrealistic signatures appearing in the results and high rejection rates of observations due to the applied outlier threshold and quality control are found in the assimilation experiments. This paper furthermore discusses the limitations of the model and the impact of ensemble member creation approaches on the assimilation results, and proposes possible methods to avoid these problems for future work.

ITIT-06 Voice and data communication system based on Software-Defined Radio technology to establish VHF radio links via Equatorial Electrojet
- by Ricardo Farino Alonso

Status of First Author: Student NOT in poster competition, Undergraduate

Authors: Ricardo Alonso, ricardo.alonso@jro.igp.gob.pe
Nadia Yoza, nadia.yoza@jro.igp.gob.pe
Ramiro Yanque, ramiro.yanque@jro.igp.gob.pe
Marco Milla, marco.milla@jro.igp.gob.pe
Jorge Chau, jorge.chau@jro.igp.gob.pe

Abstract: The Equatorial Electrojet (EEJ) is a horizontal electron current flowing along the magnetic Equator at 100 km altitude in the ionosphere. The EEJ can be used as a scattering media to establish radio communication links in the VHF band. The aim of this work is to design and implement a new communication system, based on the Software-Defined Radio (SDR) technology, to establish a point-to-point VHF radio link using the Equatorial Electrojet as the communication channel. The use of SDR technology will allow the study of the EEJ as communication channel and will improve voice and data communications using new modulation schemes and diversity techniques, which will be implemented in software, in a flexible way and without the need of additional hardware.

ITIT-07 A two-dimensional minimum mean-square error approach to Fabry-Perot interferometer analysis - by Thomas W Gehrels

Status of First Author: Student IN poster competition

Authors: Thomas W. Gehrels - U of Illinois - gehrels2@illinois.edu, Brian Harding - U of Illinois - bhardin2@illinois.edu, Jonathan J. Makela - U of Illinois - jmakela@illinois.edu

Abstract: A two-dimensional approach to the analysis of Fabry-Perot interferometer fringe patterns is presented. The two-dimensional etalon instrument function is modeled using minimum mean-square error estimation of the multi-order interferogram generated by a frequency-stabilized monochromatic laser source. The two-dimensional sky interferograms are modeled using minimum mean-square error estimation of the convolved source emission and instrument function. This approach is compared to commonly used methods, including one-dimensional and weighted-averaging techniques. Measurements from co-located

FPI systems are compared in order to verify that the computed source spectrum is independent of the instrument function

ITIT-08 Extended duration high-speed auroral tomography system
- by Michael Hirsch

Status of First Author: Student IN poster competition

Authors: Michael Hirsch, Hanna Dahlgren, Joshua Semeter
mhirsch@bu.edu, hannad@bu.edu, jls@bu.edu

Abstract: We present system design details and initial test results of a new high-speed auroral tomography system intended for high-latitude auroral arc measurements. G.P.S. receivers are used to synchronize inter-site image acquisition to measured accuracy of less than 1 millisecond. Since sustained data rates beyond 300 Megabytes per second per camera are anticipated, it is necessary to implement a reliable triggering system for auroral arc detection so that hard drive storage at remote locations is not quickly exhausted with undesired observational data. We demonstrate the utility of optical flow techniques to reliably determine when an auroral arc event of interest is occurring.

ITIT-09 Ionospheric Scintillation Monitoring Using GPS based Space Weather Monitor - by Irfan Azeem

Status of First Author: Non-student, PhD

Authors: Irfan Azeem, Geoff Crowley, Adam Reynolds, Gary S. Bust, Rick Wilder, ASTRA, Boulder CO
Jorge Chau, Jicamarca Radio Observatory
Brady W. O'Hanlon, Mark L. Psiaki, Steven Powell, Cornell University, Ithaca NY
Todd E. Humphreys, Jahshan A. Bhatti, The University of Texas, Austin TX

Abstract: Ionospheric weather includes gradients and irregularities that affect transionospheric UHF and L-band line-of-sight propagation (scintillation) and VHF/HF sky-wave and scatter propagation. Such disturbances lead to communication and navigation outages with operational impacts. These disruptive phenomena occur frequently in the tropics, less frequently in the polar region, and even less frequently at mid-latitudes, but they occur everywhere with serious consequences. However, forecasting these events remains a challenge due to insufficient ionospheric data to adequately specify the global ionosphere. The main reasons for the data scarcity are: (1) existing instruments are inadequate; (2) existing instruments are too expensive; (3) 70% of the earth is covered in water, making instrument deployment difficult. The development of tools to enable "actionable" ionospheric weather forecasts and specification of irregularities is the ultimate goal of ASTRA LLC, and development of a new real-time software-defined GPS receiver is part of the strategy. The Connected Autonomous Space Environment Sensor (CASES) GPS receiver, developed by ASTRA in collaboration with Cornell University and University of Texas, Austin, is a software-defined GPS receiver for the L1 C/A and L2C codes specifically designed as a low-cost space weather instrument for monitoring ionospheric scintillation and total electron content. In particular the CASES tracking loops permit continued tracking through deep scintillation where other receivers would lose lock. A CASES GPS receiver has been operating continuously at Jicamarca Radio Observatory, Peru (11.952S, 76.876W) since November 2011. In this paper we describe the variations in the S4 scintillation parameter as measured by the CASES GPS receiver over many months. Amplitude scintillation results show elevated values between 18 LT and 24 LT and also reveal some seasonal dependence. The CASES results are presented to demonstrate its capability to serve as low cost space weather monitor for the space physics and GPS communities.

ITIT-10 Ampules: A New Type of Sounding Rocket Payload for the Measurement of Three- Dimensional, Neutral Winds and Gradients in the Lower Thermosphere - by Carl Andersen

Status of First Author: Student IN poster competition, PhD

Authors: Carl Andersen, Mark Conde, Miguel Larsen

Abstract: A new type of sounding rocket payload for measuring neutral winds and gradients in the lower thermosphere was launched from Poker Flat, AK on February 9, 2010 and Wallops Island, VA on August 3, 2010. The payload consists of a collection of sub-payloads, or ampules, that are propelled laterally out of the rocket during flight. Each ampule contains approximately 380 ml of liquid tri-methyl aluminum (TMA) which, after separating from the main rocket, is dispersed by explosive detonation. The result is a luminous "puff" that can be tracked by triangulation using images taken from several ground stations, producing wind vector velocities with typical uncertainties of just 1-2 m/s. Future missions would deploy a constellation of TMA puffs throughout a 3-dimension volume spanning approximately 100x100 km horizontally and vertically from 100 to 180 km altitude. The objective of these deployments is to measure height profiles of all nine first-order spatial gradients of the neutral wind vector in the lower thermosphere.

ITIT-11 Further Comparison of RAIDS observations to radar-fed model of OII 83.4 nm emission - by Ewan S. Douglas

Status of First Author: Student NOT in poster competition

Authors: E. S. Douglas, S. M. Smith, A. W. Stephan, L. Cashman, S. Chakrabarti, R. L. Bishop, S. A. Budzien, A. B. Christensen, and J. H. Hecht

Abstract: We test the utility of the OII 83.4 nm emission feature as a measure of ionospheric parameters. Observed with the Remote Atmospheric and Ionospheric Detection System (RAIDS) EUV Spectrograph on the International Space Station (ISS), limb profiles of 83.4 nm emissions are compared to predicted dayglow emission profiles from a theoretical model incorporating ground-based electron densities profiles. Observations and models are compared for periods of conjunction, closely matching the model morphology and demonstrating that 83.4 nm emission is sensitive to changes in the ionospheric density profile from the 340 km altitude of the ISS during solar minimum.

ITIT-12 Helium Resonance Fluorescence LIDAR - by Tony Mangogna

Status of First Author: Student IN poster competition, PhD

Authors: Tony Mangogna, mangogni@illinois.edu; Gary Swenson, swenson1@illinois.edu; Peter Dragic, p-dragic@illinois.edu; University of Illinois Urbana-Champaign

Abstract: The Helium Resonance Fluorescence LIDAR is designed to resonantly scatter photons from helium atoms in the metastable 23S state, which sparsely populate the thermosphere. The He LIDAR will utilize a high power narrow linewidth laser and a large aperture telescope in a bistatic configuration. Simulations are used to determine expected signal returns and make comparisons between different receiver systems, including large aperture astronomical instruments.

ITIT-13 Dynamic Ionosphere Cubesat Explorer (DICE): Early Science Instrument Results - by Geoff Crowley

Status of First Author: Non-student

Authors: G. Crowley-1, C. Swenson-2, C. Fish-2, I. Azeem-1, M. Pilinski-1 , A. Barjatya-3 , G. Bust-1, M. Larsen-4, USU Student Team-2

1-ASTRA LLC., Boulder, CO
2-SDL/USU, Logan, UT
3-Embry-Riddle, Daytona Beach, FL
4-Clemson University, Clemson, SC

Abstract: The DICE mission consists of two identical 1.5U CubeSats deployed simultaneously from a single P-POD (Poly Picosatellite Orbital Deployer) into the same orbit. DICE was selected for flight under the NSF "CubeSat-based Science Mission for Space Weather and Atmospheric Research" program. The DICE twin satellites were launched on a Delta II rocket on October 28, 2011. The satellites are flying in a "leader-follower" formation in an elliptical orbit which ranges from 820 to 400 km in altitude. Each satellite carries a fixed-bias DC Langmuir Probe (DCP) to measure in-situ ionospheric plasma densities, a science grade magnetometer to measure DC and AC geomagnetic fields, and an Electric Field Probe (EFP) to measure DC and AC electric fields. These measurements will permit accurate identification of storm-time features such as the SED bulge and plume, together with simultaneous co-located electric field measurements which have previously been missing. The mission team combines expertise from ASTRA, Utah State University/Space Dynamics Laboratory (USU/SDL), Embry-Riddle Aeronautical University and Clemson University.

The DICE CubeSat mission has three scientific objectives: (1) Investigate the physical processes responsible for formation of the midlatitude ionospheric Storm Enhanced Density (SED) bulge in the noon to post-noon sector during magnetic storms; (2) Investigate the physical processes responsible for the formation of the SED plume at the base of the SED bulge and the transport of the high density SED plume across the magnetic pole; (3) Investigate the relationship between penetration electric fields and the formation and evolution of SED.

In this poster, the science mission design and status as well as the instruments making up the core science mission will be reviewed. An overview of the early science data collected by DICE will be given. The plan for continued science operations and future data processing is provided.

ITIT-14 The effects of 3D error covariance and background model bias for an ionospheric data assimilation model - by Chi-Yen Lin

Status of First Author: Student IN poster competition

Authors: C. Y. Lin

Cooperative Institute for Research in Environmental Sciences, University of Colorado, Boulder, Colorado, USA

Space Weather Prediction Center, National Oceanic and Atmospheric Administration, Boulder, Colorado, USA

Institute of Space Science, National Central University, Jhongli, TAIWAN

T. Matsuo

Cooperative Institute for Research in Environmental Sciences, University of Colorado, Boulder, Colorado, USA

Space Weather Prediction Center, National Oceanic and Atmospheric Administration, Boulder, Colorado, USA

E. A. Araujo-Pradere

Cooperative Institute for Research in Environmental Sciences, University of Colorado, Boulder, Colorado, USA

Space Weather Prediction Center, National Oceanic and Atmospheric Administration, Boulder, Colorado, USA

J. Y. Liu

Institute of Space Science, National Central University, Jhongli, TAIWAN

National Space Organization, Hsinchu, TAIWAN

Abstract: NOAA/SWPC data assimilation model for the ionosphere is based on the Gauss- Markov Kalman filter with the International Reference Ionosphere (IRI) as the background model, with the electron

density profiles described in terms of a handful of Empirical Orthogonal Functions (EOF). To obtain assimilative analyses over the Northern America, EOF coefficients at a given longitude- latitude grid location are inferred from ground-based GPS total electron content (TEC) data by using a Kalman filter. The model has been proved to have an accuracy of about 2 TECu (1016 #/cm²) on average over CONUS, when used for ground-based GPS data. However, we have found that the model is not suited to assimilate FORMOSAT- 3/COSMIC (F-3/C) GPS occultation TEC data. Due to the fact that occultation observation paths pass through large longitude latitude areas at different altitudes, the original EOF-based method with 2D background error covariance cannot be applied to occultation data. To overcome the limitation of the EOF-based method, we used the 3D background error covariance to assimilate both space-based F-3/C occultation data and ground-based GPS observation data. Moreover, we have found that IRI shows regional biases with respect to F-3/C occultation TEC and ground-based GPS observation TEC. The bias correction is also an important issue to increase the accuracy of the assimilation result. We characterize regional IRI background model biases, by comparing simulated synthetic TEC to the two sets of GPS data: F-3/C occultation and ground-based GPS data.

ITIT-15 Estimation of Vertical Drifts using Magnetometer Data with Neural Network - by Percy Jesus Condor Patilongo

Status of First Author: Student NOT in poster competition

Authors: Percy J. Condor P.

Abstract: We can estimate the magnitude of vertical ExB drifts in the F-region Ionosphere using magnetometer data with Neural Network. In this work we use the magnitude of the horizontal (H) component of B measured for magnetometers at Jicamarca Radio Observatory and Piura (Peru) from 2002 to 2009. A parameter used in the training with Neural Network (NN) is the difference in the magnitudes of H between JRO (placed on the magnetic equator) and Piura (displaced more 5° away) (dH). Also others parameters used are indexes F10.7 and Ap. The estimation with NN is very good. We have an RMS error of 3.7 m/s in the estimation using dH and 3.9 m/s when we use the component H of JRO. The results are validated using set of vertical drifts observations from the Jicamarca incoherent scatter radar (ISR) located at Peru. This estimation is shown on the website: <http://jro-app.igp.gob.pe/driftnn>, where we can get vertical drifts of F-region Ionosphere online for JRO. Then it can be a useful tool for researchers in Upper Atmosphere.

ITIT-16 Extended SAMI2 Model in a Double Adiabatic form - by Liyuan Mei

Status of First Author: Student IN poster competition, PhD

Authors: Liyuan Mei, li.yuan.mei@dartmouth.edu

Abstract: Grad's 20 moment transport equations can be simplified to a set of six partial differential equations under the limit of strong external magnetic fields and with the assumption of E*B convection. The set of six equations can be further reduced to four (continuity, momentum, parallel and perpendicular pressure equations) with the assumption that heat flow is negligible except in the presence of frequent collisions. In this case, the four equations are closed by expressions for parallel and perpendicular heat flux due to collisional transport (Gombosi and Rasmussen, 1991). This set of equations is used to extend the SAMI2 model of the Ionosphere (Huba et al., 2000) to a double adiabatic form that models plasma along a flux tube from northern hemisphere to southern hemisphere. In the extended model, the continuity equation remains unchanged and is solved for seven ion species (H⁺, He⁺, N⁺, O⁺, N₂⁺, NO⁺, and O₂⁺). Mirror forces are added in the parallel ion momentum equations. Parallel and perpendicular pressure equations are solved for H⁺, He⁺, O⁺ and electrons. As in the original SAMI2 model, motions are assumed to E*B drift. The extended SAMI2 model reveals the importance of pressure anisotropy in the ionosphere, and it enables further study of transversely heated ion outflows in the high latitude ionosphere.

ITIT-17 The effects of Coulomb collisions on H⁺, He⁺, and O⁺ plasmas for incoherent scatter radar applications at Jicamarca - by Marco Antonio Milla

Status of First Author: Non-student, PhD

Authors: Marco Milla (marco.milla@jro.igp.gob.pe) 1

Erhan Kudeki (erhan@illinois.edu) 2

Daniel Suárez (daniel.suarez@jro.igp.gob.pe) 1

Jorge Chau (jorge.chau@jro.igp.gob.pe) 1

1 Radio Observatorio de Jicamarca, Instituto Geofísico del Perú, Lima, Perú

2 Department of Electrical and Computer Engineering, University of Illinois at Urbana-Champaign, Urbana, IL

Abstract: The need for considering the effects of Coulomb collisions in modeling the spectrum measurements at Jicamarca was first suggested by Sulzer and González [1999]. Motivated by this work, Milla and Kudeki [2011] developed a collisional spectrum model that takes into account Coulomb collision effects at all magnetic aspect angles including the direction perpendicular to B as needed for Jicamarca applications. The model has been applied in preliminary fittings of radar data providing encouraging results. However, the model was developed only for O⁺ plasmas, which limits its application to F-region measurements between 200 km and 600 km. As an extension of this work, we are in the process of developing a new multi-component collisional incoherent scatter spectrum model that considers O⁺, H⁺, and He⁺ plasmas as needed for perpendicular-to-B radar observations at Jicamarca. The development of the spectrum model is being carried out based on the simulation of charged particle trajectories embedded in a collisional magnetized plasma. In our approach, friction and diffusive forces model the effects of Coulomb collisions on the particle motion; the expected values of these forces are taken from the standard Fokker-Planck model of Rosenbluth et al. [1957]. Since the simulation process is a very demanding computational task, we have developed a CUDA-based simulation program in order to run the simulations in an NVidia Tesla GPU system. The detailed study of the statistics of the simulated trajectories will give us further insight into the physics of Coulomb collisions, which is needed for the interpretation of incoherent scatter measurements. For instance, we have found that the motion process of the ions can be approximated as a standard Brownian motions process, and thus analytical expressions for ion statistics functions can be determined. On the other hand, in the case of the electrons, their motion is more complicated than a Brownian process and requires a detail analysis, however, a simplification is possible since the characteristics of the electron motion are independent from the type of plasma considered. In this presentation, we will report on our advances on the development of this new spectrum model. The model will be used in the simultaneous estimation of drifts, densities, and temperatures of the equatorial ionosphere in perpendicular-to-B experiments at Jicamarca. This experimental evaluation will have a broader impact since the accuracy of the Fokker-Planck collision model will be tested.

ITIT-18 Comparison of Time Domain and Frequency Domain Analysis to Estimate Velocity Profile of Field-Aligned Plasma Irregularities - by Ramin Jafari

Status of First Author: Student IN poster competition, Masters

Authors: Ramin Jafari (1), Bill Bristow (2)

Abstract: The SuperDARN FITACF algorithm analyses the autocorrelation function of the received RADAR backscatter to estimate power, velocity and spectral width of the field-aligned plasma irregularities. Frequency domain techniques such as Fourier transform and Lomb periodogram can be applied to derive the same parameters. In comparison to spectral analysis, the FITACF algorithm has higher resolution in estimating Doppler velocity, but it fails when there are several moving targets or ground scatter in the same range. In addition, missing or bad lags in the lag profile result in unequally-spaced data. Hence, Fourier transform fails. Lomb periodogram, which uses least square fitting of sines and cosines to extract frequency components in non-uniformly spaced data, can be applied. Each method and its trade-offs were studied and examples are provided which show the superior performance of frequency domain analysis over the current algorithm.

ITIT-19 Particle Image Velocimetry (PIV) measurements of the vector velocity of equatorial spread F irregularities over Jicamarca - by Juan Miguel Urco

Status of First Author: Student NOT in poster competition, Undergraduate

Authors: Juan Urco, miguel.urco@jro.igp.gob.pe and Jorge Chau, jorge.chau@jro.igp.gob.pe

Abstract: Since the first report made in 1938, Equatorial Spread F (ESF) has been observed with great interest. At Jicamarca, this phenomenon has been observed continuously by the main radar operating in the CSR (Coherent Scatter Radar) mode since 1996 and recently a new mode of operation, called JULIA Imaging, have been implemented. This new mode provides ESF data with high resolution in altitude, space, and time.

In this work, taking advantage of the similarity between the behaviour of ESF turbulence and fluid turbulence, and due to the horizontal velocity is unknown; we will use the particle image velocimetry (PIV) technique to estimate the 2-D velocity field measurements of the imaging data. Among other procedures, we will use two interrogation images separated by a known time that will be correlated to obtain the plasma displacement between two images.

**ITIT-20 A 50-MHz Digital Radar System for Ionospheric Studies
- by Alexander Hackett**

Status of First Author: Student IN poster competition, Masters

Authors: Alexander Hackett - Pennsylvania State University
Robert Sorbello - Pennsylvania State University
Dr. Julio Urbina - Pennsylvania State University
Dr. Erhan Kudeki - University of Illinois
Dr. Steven Franke - University of Illinois

Abstract: The Cognitive Interferometry Radar Imager (CIRI) is an advanced 50-MHz digital radar system designed to study ionospheric plasma phenomena. Being entirely software-controlled, many advanced feature possibilities exist, including the currently implemented remote start/stop capability and automatic generation of range-time-intensity (RTI) plots at regular intervals. The CIRI@Andes system in place at Observatorio de Huancayo, Peru was derived from the IRIS/RITA system currently in operation at the University of Illinois. Preliminary observations of the equatorial electrojet and meteors taken in Huancayo show promising results. Continued collaboration between the teams at Penn State University and the University of Illinois is planned to improve and expand upon the existing system hardware and software.

Long-Term Variations of the Upper Atmosphere

LTRV-01 Inter- and Intra-Annual Variability of Tidal Components Observed in FORMOSAT-3/COSMIC TECs, 2007-2011 - by Loren Chang

Status of First Author: Non-student

Authors: Loren C. Chang
Department of Earth Sciences, National Cheng Kung University, Tainan, Taiwan
Charles C.H. Lin
Department of Earth Sciences, National Cheng Kung University, Tainan, Taiwan
Jann-Yenq Liu
Institute of Space Science, National Central University, Jhongli, Taiwan

Abstract: Tidal decomposition of ionospheric fields can be a useful tool for isolating and understanding specific features and mechanisms generated in-situ, or related to coupling from other atmospheric regions. In this study, we present zonal mean and major tidal components retrieved from FORMOSAT-3/COSMIC observations of low to mid latitude TEC from 2007-2011. The spatial features, seasonal, and inter-annual variability of these components are discussed in the context of their relation to ionospheric variability as a whole.

LTRV-02 The effects of changes in the Earth's magnetic field on the magnetosphere, ionosphere and thermosphere - by Ingrid Cnossen

Status of First Author: Non-student, PhD

Authors: Ingrid Cnossen, Arthur D. Richmond, Michael Wiltberger
High Altitude Observatory, National Center for Atmospheric Research, Boulder, CO, USA

Abstract: The Earth's magnetic field changes in orientation and strength over time. We study the response of the magnetosphere, ionosphere and thermosphere system to such changes using the Coupled Magnetosphere-Ionosphere-Thermosphere (CMIT) model. A decrease in dipole moment causes the magnetosphere to shrink and also changes its shape. The ionospheric conductance strongly increases with decreasing dipole moment. This results in stronger field-aligned currents and a weaker electric field in the high-latitude ionosphere. ExB drifts scale as E/B and initially increase with increasing dipole moment, but then decrease. This leads to similar behaviour in the Joule heating, the global mean exospheric temperature, and the height of the peak of the F2 layer, h_mF2 . The peak electron density of the F2 layer shows the opposite behaviour, which is associated with changes in circulation affecting the balance between ion loss and production. Changes in tilt angle, somewhat surprisingly can also cause global mean changes in thermospheric temperature and electron density. A higher tilt angle, on average, leads to a diminished coupling between the solar wind and the magnetosphere, which causes this effect. There are also strong changes in spatial patterns as a function of dipole moment for any variables that are normally organized in magnetic latitude. Diurnal and seasonal variations also change.

LTRV-03 Investigation of Solar Cyclic and Climatic Trends in Upper Atmospheric Hydrogen Distributions - by Susan M. Nossal

Status of First Author: Non-student

Authors: S. Nossal, Physics Dept., University of Wisconsin-Madison
E. J. Mierkiewicz, Physics Dept., University of Wisconsin-Madison
F.L. Roesler, Physics Dept., University of Wisconsin-Madison
L. Qian, High Altitude Observatory, National Center for Atmospheric Research
S. Solomon, High Altitude Observatory, National Center for Atmospheric Research
A. Burns, High Altitude Observatory, National Center for Atmospheric Research

Abstract: We will discuss work in progress to better understand solar cyclic and climatic influences on hydrogenous species budgets and distributions from both an observational and modeling perspective. Our Fabry-Perot observations of upper atmospheric hydrogen emissions during solar cycle 23 and during three solar minima (1985, 1997, 2006-2008) establish a reference data set of highly precise, consistently calibrated, thermospheric + exospheric hydrogen column emission observations from Northern mid-latitudes that can be used to compare with future observations and with atmospheric models. We will also discuss use of the NCAR global mean model for sensitivity studies to investigate the response of thermospheric hydrogen to a doubling of carbon dioxide and methane. The results from this study suggest a strong solar cycle dependence and that carbon dioxide cooling may have a greater impact upon the changes in the upper atmospheric hydrogen distribution than do methane increases.

Midlatitude Ionosphere or Thermosphere

MDIT-01 GPS TEC measurements at Clemson, SC, during Solar Minimum - by Jonathon Nooner

Status of First Author: Student IN poster competition

Authors: Jonathon Nooner, jnooner@clemson.edu

Abstract: Measurements with a single dual frequency GPS receiver were taken in Clemson South Carolina and have been used to compute the total electron content (TEC) of the ionosphere. To address the difficulty of estimating the receiver bias with a single station, the data collected at Clemson is calibrated with data extracted from JPL's global TEC maps. The data set is analyzed for events of solar activity and midlatitude ionospheric disturbances. Analysis of this data is accomplished, in part, through use of GPStk, an open source c++ library.

MDIT-02 Ground-based GPS Observation of SED-associated Irregularities Over CONUS - by Yang-Yi Sun

Status of First Author: Student IN poster competition

Authors: Yang-Yi Sun, Tomoko Matsuo, Eduardo A. Araujo-Pradere, and Jann-Yenq Liu

Abstract: It has been known that steep total electron content (TEC) gradients observed at the boundary between the storm-enhanced plasma density (SED) and the ionospheric trough at sub-auroral and mid-latitude regions are associated with ionospheric irregularities that in turn impact communication and navigation systems. However, the relationship between the SED-associated irregularities and TEC gradients is still not well understood, partly because of the difficulties of resolving small-scale TEC gradients from sparsely distributed TEC observations. In this study we examine the relationship between the SED-associated irregularities and TEC gradients during the intense geomagnetic storms of March 31, 2001 and October 30, 2003. TEC maps over the continent of United States (CONUS) are constructed from ground-based GPS TEC data, using Kalman filter update formulas with a recently developed nonstationary wavelet-based error covariance model that enables resolution of TEC gradients on finer scales. Our results show that both large-scale TEC gradients and the zonal ion drift play an important role in the formation of irregularities at the boundary between SED and mid-latitude low TEC regions, where favorable conditions for the plasma instability (i.e. $(\mathbf{E} \times \mathbf{B}) \cdot \nabla n > 0$, based on the linear theory of Rayleigh-Taylor instability) are satisfied. Furthermore, our results show that small-scale latitudinal TEC gradients are related to the formation of SED-associated irregularities within the low TEC region.

MDIT-03 Comparing A Simulated Plasmasphere Using Different Driving Electric Field Models With IMAGE EUV Data - by Aron Dodger

Status of First Author: Student IN poster competition, PhD

Authors: Aron Dodger

Abstract: The plasmasphere is a region of low-energy, high-density plasma in the inner magnetosphere. This region controls the mass density of the inner magnetosphere, and is important in considering the waveparticle interactions responsible for energy transfer in the overlapping ring current and radiation belts. The plasmasphere is a very dynamic region that is most significantly controlled by the ionospheric electric fields mapped out along the magnetic field lines. This poster compares the use of a number of electric field models to drive a plasmasphere model, specifically the Dynamic Global Core Plasma Model (DGCPM). The results of these field models will be compared against IMAGE EUV plasmopause positions for a selection of storm events. A number of different plasmopause identification methods are employed to determine a best fit method to IMAGE EUV data.

MDIT-04 Model Simulation Of E Region Electron Density and Sporadic E Layers -
by Yen-Chieh Lin

Status of First Author: Student IN poster competition

Authors: Yen-Chieh Lin

Abstract: In this study, we not only simulate height-time variations of background electron density of E region ionosphere but also study the formation of Sporadic E layers that is highly associated with the neutral wind shear. In order to model the electron density of E region, we calculate the densities of NO^+ , O_2^+ , N_2^+ , O^+ , Fe^+ that are assumed to consist in the ions in E region. The initial condition of the simulation is the photochemical equilibrium in E region, we calculate theoretical production rate and loss rates of the ions and substitute them into continuity equation to solve the first-order partial differential equation in accordance with Runge-Kutta method.

We then model the tidal wind that is responsible for the formation of Sporadic E layers. In the lower E region, the zonal neutral wind is the primary factor causing vertical ion drifts, which is the physical process of $\mathbf{U} \times \mathbf{B}$ dynamo in E region. Therefore, it requires that the zonal neutral wind with westward in upper and eastward in the lower E region will result in ion convergence in northern hemisphere. The Sporadic E layers will occur at the region where the ion converges. With this configuration, the vertical ion drift velocity induced by tidal wind constitutes the transport term in continuity equation. Once the transport term is considered in the continuity equation, we use the Crank-Nicholson method to solve the resulting partial differential equation. The result indicates that a sporadic E layers indeed occurs at the regions where the ion are converged in the node of the neutral wind shear.

MDIT-05 Inter-hemispheric and latitudinal comparisons of MTM characteristics
- by Dustin Hickey

Status of First Author: Student IN poster competition

Authors: C. Martinis, A. Wright, B. Oliver, L. Goncharenko, L. Condori, J. Chau, N. Aponte, C. Brum

Abstract: We are conducting a study to look for evidence of the midnight temperature maximum (MTM) with incoherent scatter radar (ISR) data from the Jicamarca Radio Observatory, Peru (-11.95° , 283.13°). and the Millstone Hill Observatory, USA (42.62° , 288.51°). The MTM is a local maximum in the neutral temperature around midnight. Variations in the nighttime plasma temperatures T_e and T_i , determined by ISR techniques, should reflect variations in the neutral temperature T_n . We characterize the MTM in terms of amplitude, time of occurrence and width. We have just completed a comprehensive study of the MTM at 300 km using the Arecibo ISR (18.35° , 293.25°) that allowed us to determine seasonal patterns in amplitude and local time of occurrence. Jicamarca's latitude is similar to Arecibo, but in the opposite hemisphere. A total of 185 nights with Jicamarca ISR data will be analyzed. Preliminary results indicate MTM detections but at a much earlier local time when compared with Arecibo. We will also use Millstone Hill ISR to specifically look at low elevation angle runs that allow the determination of thermospheric T_i near $25-30^\circ$ GLAT. Specific dates when the MTM was observed at Arecibo will be analyzed. A total of 48 nights of data were found when Millstone Hill was running at low elevations and there was an MTM at Arecibo.

MDIT-06 Atmospheric and ionospheric waves disturbed from the rocket source
detected by a Taiwanese GPS array - by Jia-Ting Lin

Status of First Author: Student IN poster competition, Masters

Authors: J. T. Lin

Institute of Space, Astrophysical and Plasma Sciences, National Cheng Kung University, Tainan, Taiwan
C. H. Lin, C. H. Chen

Department of Earth Science, National Cheng Kung University, Tainan, Taiwan

Y. Y. Sun, J. Y. Liu

Institute of Space Science, National Central University, Chung-Li, Taiwan

W. H. Chen

Department of Earth Science, National Cheng Kung University, Tainan, Taiwan

Abstract: The exhaust plume of the rocket is a very powerful source of energy that excites atmospheric acoustic perturbations. Because of the coupling between neutral particles and electrons at ionospheric altitudes, these acoustic perturbations induce variations of the ionospheric electron density. We detected the ionospheric perturbations by a Taiwanese dense array of global positioning system (GPS) receivers when the carry rocket of Cheng'E 2 satellite pass through the ionospheric altitudes above Taiwan. These perturbations include the abruptly decrease of TEC due to neutral water vapor from the exhaust plume, and the oscillatory signature.

Owing to an dense array of GPS, after a high-pass filter, it clearly shows the first impulsive of bow wave front propagating along horizontal direction, follow by a oscillatory guided wave.

MDIT-07 Investigation of the parallel transport scheme in SAMI2

- by Timothy M. Duly

Status of First Author: Student IN poster competition Masters

Authors: Duly, T. M., Huba, J. D. (huba@ppd.nrl.navy.mil), Makela J. J. (jmakela@illinois.edu)

Abstract: In this poster, the parallel transport scheme of SAMI2 (Sami Is Another Model of the Ionosphere) is investigated. SAMI2 utilizes a first order, finite volume, implicit donor cell method to transport plasma along the magnetic field lines. It was designed to be diffusive in order to placate potential spurious numerical oscillations within the model. However, for some instances (i.e., for medium-scale traveling ionospheric disturbances (MSTID) seed development), a higher order scheme is required to maintain random perturbations. Here, we investigate a second order, total variation diminishing (TVD) scheme and implement it into SAMI2. A test case of random perturbation (indicative of MSTID seeding) and the results between the two schemes are compared. Finally, a short discussion of the trade-offs between the two schemes is given.

MDIT-08 Modeling of the Weddell Sea Anomaly: Effects of thermospheric wind

- by Levan Lomidze

Status of First Author: Student IN poster competition, PhD

Authors: Levan Lomidze and Ludger Scherliess

Center for Atmospheric and Space Sciences, Utah State University, 4405 Old Main Hill, Logan, UT 84322

Abstract: The Weddell Sea Anomaly (WSA) is a mid-latitude F region ionosphere phenomena taking place over the regions west of the Antarctic Peninsula. It is most prominent during local summer and is characterized by larger electron densities at night than at noon. Though the WSA has been known for several decades, its generation mechanism is not fully understood and its modeling remains a challenge. In the current study the radio occultation measurements from the six FORMOSAT-3/COSMIC satellites combined with a physics-based data assimilation model of the ionosphere were used to understand the role of thermospheric winds on the WSA generation. The data assimilation model is the Global Assimilation of Ionospheric Measurements Full-Physics model (GAIM-FP) that covers the altitude range from 90 to 20,000 km, includes six ion species, and allows for inter-hemispheric flow. As an output, it provides the 3-dimensional density distribution throughout the ionosphere and information about the physical drivers, including the magnetic meridional wind. To establish the effects of the thermospheric wind on the WSA generation, model runs were performed with empirical winds and with GAIM-FP calculated winds. In order to better understand the responsible mechanisms we developed a method to decouple the magnetic

meridional wind into its geographic meridional and zonal components and separately analyzed their effects on the anomaly. The calculated neutral wind components were also compared with HWM93 and HWM07 empirical winds.

MDIT-09 Neutral wind effect on mid-latitude summer nighttime anomaly
- by Fu-Yuan Chang

Status of First Author: Student IN poster competition, PhD

Authors: Fu-Yuan Chang, fychang1228@gmail.com

Abstract: The Weddell Sea Anomaly (WSA) is most pronounced feature in the southern summer hemisphere, where the electron density in the Weddell Sea region becomes the greatest during the nighttime period. In this paper, we using electron density profiles derived by the GPS radio occultation experiment on board FORMOSAT-3/COSMIC (F3/C) satellites examine the WSA feature at various global fixed local times from February 2009 to January 2010. It is found that the WSA feature moves eastward daily, and appears in various seasons except winter of the southern hemisphere. Simulations of Horizontal Wind Model 2007 (HWM07) indicate that the magnetic meridional wind plays an important rule.

MDIT-10 Simultaneous Fabry-Pérot interferometer observations of thermospheric winds and dynamics at the Pisgah Astronomical Research Institute and at the Millstone Hill Optical Observatory - by Samuel Sanders

Status of First Author: Student IN poster competition

Authors: J. Meriwether, M. Castelez, J. Noto, R. Kerr, S. Kapali, M. Migliozi, J. Riccobono, J. Makela, D. Fisher

Abstract: Coincident Fabry-Pérot interferometer (FPI) observations obtained at the Pisgah Astronomical Research Institute (PARI; 35.20 N, 82.88 W) in North Carolina and at the MIT optical facility at Millstone Hill Observatory (MHO; 42.62 N, 71.49 W) during the winter of 2011-2012 have revealed a nighttime temperature peak similar to that observed at lower latitudes and identified as the midnight temperature maximum (MTM). In several instances two peaks were seen, one at ~21 LT and the other at ~03 LT, with amplitudes of 20-25 K and 75-100 K, respectively. The zonal and meridional thermospheric winds for both locations are similar in behavior, featuring eastward winds during the evening followed by a meridional southward surge in the early morning hours before dawn. The zonal winds for the PARI location were generally larger by ~50 ms⁻¹, and the meridional winds weaker by ~25-50 ms⁻¹ relative to MHO zonal and meridional winds, respectively.

MDIT-11 Analytical solution of the neutral dynamic stability problem to characterize irregularities at midlatitude sporadic E layers - by Eliana Nossa

Status of First Author: Student NOT in poster competition

Authors: Eliana Nossa (1) and David Hysell (2)

(1) Departments of Electrical and Computer Engineering and Earth and Atmospheric Sciences, Cornell University, Ithaca, NY
(en45@cornell.edu)

(2) Department of Earth and Atmospheric Sciences, Cornell University, Ithaca, NY

Abstract: An analysis of neutral shear flow associated with midlatitude Es layer irregularities is presented. The equation for the dynamics of inviscid shear flows, known as the Taylor-Goldstein (TG) equation, is known to have multiple solutions. The solutions are directly related with the characteristics of the background winds. The properties of the neutral winds in the MLT region are characterized here by a modified 3D elliptic Bickley jet model, which represents the winds as a corkscrew in the region of interest

with small values outside it. Generalizing the 2D work of Drazin and Howard [1966] for the aforementioned conditions, analytical expressions for the direction of propagation, growth rate and wavelength of unstable waves are obtained when the buoyancy force is neglected. The results can be compared with known properties of Es layer irregularities. An example is presented for representative conditions. The analysis predicts a growth time of few minutes, propagation in the NE-SW quadrant and wavelengths of about 20 km. Also, a clear relationship between displacements from the origin of the background winds and the direction of propagation is shown. For displacements in the first and third quadrant, the propagation is located in the NE-SW quadrants. For displacements in the second and fourth quadrant, the displacements are in the NW-SE quadrants. The properties of the growing waves are similar to the roll-like deformations of Es layers often observed at midlatitudes.

Polar Aeronomy

POLA-01 Comparison of in situ and ground-based measurements during the MICA sounding rocket flight - by Robert Miceli

Status of First Author: Student IN poster competition, PhD

Authors: Miceli, Robert J.
Hysell, David L.
Powell, Steven P.
Hampton, Don L.

Abstract: On February 19, 2012, the MICA sounding rocket was launched from Poker Flat Research Range into an auroral substorm. Direct measurements of the electric and magnetic field were made from the sub-payload using a magnetometer and COWBOYS (Cornell Wire Boom Yo-Yo System) up to an altitude of 325 km. On the ground, data from the PFISR, a coherent scatter radar in Homer, Alaska, and optical data from several all-sky cameras was recorded before, during, and after the flight. The PFISR provided information about the ionospheric density, temperature, and line of sight velocity in the E and F-regions, and the coherent scatter radar measured the signal-to-noise ratio, Doppler shift, and Doppler width of the auroral echoes in the E-region. The PFISR gives some indication of the large-scale electric fields, while the Homer radar provides small-scale E-field measurements with higher resolution. A comparison of the flight and ground-based data sets are presented to provide a greater understanding of the plasma processes that occur during an auroral substorm.

POLA-02 Role of Ionospheric Boundary Conditions on the Evolution of Field-aligned Currents - by Tapas Bhattacharya

Status of First Author: Student IN poster competition, PhD

Authors: Tapas Bhattacharya, Antonius Otto, Dirk Lummerzheim
Geophysical Institute, University of Alaska Fairbanks

Abstract: Field-aligned current systems play an important role in transferring energy and momentum from the solar wind or from the magnetotail current sheet to the ionosphere and hence are central to the Magnetosphere-Ionosphere coupling. Specifically, it is usually considered that they play a critical role in the evolution and morphology of active discrete auroral arcs. While the driver for the formation of field-aligned currents is usually considered to be of magnetospheric origin, properties such as the ionospheric conductances and density irregularities can have a significant effect on the formation and evolution of narrow field-aligned current curtains.

We study the plasma dynamics in the framework of 3D MHD simulations using the introduction of Alfvénic perturbations in the velocity and magnetic field at the magnetospheric boundary. In this presentation we examine the generation and modifications of field-aligned currents in response to the Alfvén wave interaction with the ionosphere with emphasis on the role of different ionospheric boundary

conditions. Of particular interest are the effects of strong gradients of ionospheric conductance and their orientations with respect to the direction of perturbation.

POLA-03 Millstone Hill and Palmer Station Fabry-Perot interferometer observations
- by Qian Wu

Status of First Author: Non-student

Authors: Qian Wu, NCAR/HAO
John Noto, SSI
R. Kerr, SSI

Abstract: To understand hemispheric differences in thermosphere a pair of Fabry-Perot interferometers at Millstone Hill (54N MLAT) and Palmer station (54S MLAT) were used to observed thermospheric winds. These two stations are close to be conjugate to each other. The electric field at the two conjugate points should be similar. However, the pressure gradient and other forcings at the two locations are different. We should expect different thermospheric winds in the two hemispheres. How the ionosphere reacts to similar electric fields and different winds in the two hemispheres can be very interesting. We plan to compare the observations with the NCAR TIEGCM model simulations to examine the thermosphere ionosphere interaction in the two hemispheres. Such inter-hemispheric comparison can lead to a better understanding of the thermosphere ionosphere interaction.

POLA-04 First Daytime Thermospheric Wind observation by HIWIND - by Qian Wu

Status of First Author: Non-student

Authors: Qian Wu, HAO/NCAR
W. Wang HAO/NCAR
Ingermar Haggstrom, EISCAT
Anja Stromme, SRI

Abstract: HIWIND is the first balloon borne Fabry-Perot interferometer for day and night thermospheric wind measurements and had a very successful first flight in June 2011. High quality thermospheric wind and simultaneous EISCAT incoherent scatter radar data were obtained. Based on the combined HIWIND and EISCAT observations, the ion neutral collision frequency was estimated and thermosphere ionosphere interaction was investigated. Observations were also compared with NCAR TIEGCM simulations.

POLA-05 Simulating magnetosphere-ionosphere coupling in the TIEGCM
- by Stanley Gene Edwin

Status of First Author: Student IN poster competition, Undergraduate

Authors: Stanley G. Edwin sedwin@alaska.edu
Science Research Mentor:
Astrid Maute Ph.D., maute@hao.ucar.edu,
Art Richmond Ph. D, richmond@hao.ucar.edu

Abstract: At high latitude there is a strong coupling between the magnetosphere and ionosphere. Modeling the full coupling can require extensive computing resources, since a magnetosphere model has to be coupled to an ionosphere model. Therefore, most general-circulation models (GCMs) approximate this high-latitude coupling by using empirical models [Weimer 2005, Heelis et al. 1982] that specify the high-latitude convection pattern for different geospace conditions. This research aims not only to show the viability of the NCAR Thermosphere-Ionosphere Electrodynamics GCM (NCAR-TIEGCM) [Richmond et al., 1992] in its ability to model the magnetosphere-ionosphere coupling using a prescribed electric potential from the empirical model [Heelis et al. 1982], but also to show that it can accurately represent the coupling using field-aligned current (FAC) consistent with the prescribed electric potential. Using FAC to

drive the high latitudes has the advantage that the neutral wind effects can be considered everywhere instead of using a prescribed empirical electric-potential pattern. In addition, with new data from the AMPERE project (ampere.jhuapl.edu), the TIEGCM has the option to be driven by a more realistic spatial and temporal distribution of the energy input. This study compared the effects of forcing the model with a prescribed electric potential to forcing the model with a consistent FAC. The results indicate that convection is stronger when the model is forced by FAC because of the neutral wind effect. We further examine the difference in total energy input and its effects on the thermosphere temperature. The electric potential is affected by the FAC. Since the electric potential is changing the neutral winds are affected. In addition the Joule heating is also affected by the ion density and conductivity, and the temperature by all. Further studies would be using satellite data for the TIEGCM FAC input.

POLA-06 Field-aligned motion and morphology of fine scale breakup arcs

- by Hanna Dahlgren

Status of First Author: Non-student

Authors: H. Dahlgren(1), J. L. Semeter(1), R. A. Marshall(2), M. Zettergren(3), M. Lessard(4) and C. Weaver(4)

(1) Department of Electrical and Computer Engineering and Center for Space Physics, Boston University, Boston, Massachusetts, USA

(2) Space, Telecommunications and Radioscience (STAR) Laboratory, Department of Electrical Engineering, Stanford University, Stanford, California, USA.

(3) Physical Sciences Department, Embry-Riddle Aeronautical University, Daytona Beach, Florida, USA

(4) Space Science Center, University of New Hampshire, Durham, New Hampshire, USA

Abstract: Auroral breakup marks the start of the substorm expansion phase, when the energy stored in the magnetosphere during the substorm growth phase is unloaded to the ionosphere through Earthward high speed plasma flows. Ground-based imagers reveal a sudden explosive brightening and the auroral breakup morphology contains much fine scale structuring, with widths perpendicular to the geomagnetic field of down to 100 m or less. To fully resolve the dynamic processes of breakup arcs requires advanced high-speed optical systems with high spatial resolution.

We present unique observations of an auroral breakup event from a substorm on 1 March 2011 at Poker Flat, Alaska. The data was captured with an optical system containing a scientific CMOS detector, providing an unprecedented temporal resolution of 50 frames/s and 50 m spatial resolution. The captured images reveal apparent streaming motion of emissions along the auroral rays, so called flaming, from the edges of the imager field of view toward the center, throughout the 12 second long sequence of optical data. The details of four different flaming rays are analyzed, and comparisons with modeled emission profiles show that the energy dispersion is characteristic for Alfvénic processes. Pi1B pulsations are detected during the time sequence, and the pulsating period corresponds well with the flaming velocities, implying a magnetospheric source region rather than local acceleration.

POLA-07 An empirical model of large- and small-scale electric fields in Earth's high-latitude ionosphere - by Ellen D. P. Cousins

Status of First Author: Student IN poster competition, PhD

Authors: E. D. P. Cousins and S. G. Shepherd
Thayer School of Engineering, Dartmouth College
ellen.cousins@dartmouth.edu

Abstract: Electric fields in the high-latitude regions of Earth's ionosphere are an important component of the coupled magnetosphere-ionosphere-thermosphere system. Empirical models of these fields are useful for understanding their average behavior and for providing somewhat realistic boundary conditions to

numerical simulations of neighboring regions, such as the thermosphere. Using a large dataset of plasma drift measurements from the SuperDARN radars in both hemispheres, an empirical model that includes both large-scale average convection and spatial and temporal small-scale electric field variability is derived for the Northern and Southern hemispheres. The large-scale convection pattern varies smoothly with changing solar wind conditions and dipole tilt angles. To this convection pattern, random, small-scale fluctuations are added in such a way that the observed properties of electric field variability are approximately reproduced. The observed small-scale variability has a non-Gaussian distribution of fluctuations and has a spatial distribution that maximizes in the dayside and auroral regions and varies with dipole tilt angle and IMF clock angle. Furthermore, this small-scale variability is found to be on the same order of magnitude as (and in some cases larger than) the background fields. The new empirical electric field model is developed to be compatible with global ionosphere-thermosphere general circulation models.

POLA-08 Empirical models of Poynting flux and kinetic energy flux constructed from FAST data - by Russell Cosgrove

Status of First Author: Non-student

Authors: Russell Cosgrove and Hasan Bachivan

Abstract: Empirical models of the incident Poynting flux and particle kinetic energy flux, associated with auroral processes, have been constructed using data from the FAST satellite. The models output flux maps as a function of several geophysical parameters: (1) clock angle of the interplanetary magnetic field (IMF), (2) magnitude of the IMF in the GSM y-z plane, (3) solar wind speed, (4) solar wind number density, (5) magnetic dipole tilt angle, and (6) the Al index. The choice of parameters is motivated by the Weimer potential model. The models have been constructed by fitting the FAST data set to a sum of basis functions, with coefficients modeled by quadratic equations in the geophysical parameters. The basis functions are constructed from the FAST data set using singular value decomposition, along with a smoothing/interpolation algorithm that minimizes curvature and incorporates uncertainty. The models will soon be made available online.

POLA-09 A new branch of the ionospheric feedback instability: Importance to E region physics - by Russell Cosgrove

Status of First Author: Non-student

Authors: Russell Cosgrove and Rick Doe ,SRI International

Abstract: Rocket measurements of E region wave electric fields show that the amplitude of meter-scale waves is not sufficient to account for the observed heating of electrons, and that longer wavelength waves must be important in the auroral ionosphere [Bachivan and Cosgrove, 2010]. These longer wavelength waves have hardly been studied. The dispersion relations for the Farley Buneman and gradient drift instabilities were originally derived with the equatorial ionosphere in mind, where the magnetic field (B) lines extend for hundreds of kilometers without changing altitude by more than a kilometer. Although these instabilities have been assumed to apply in a qualitative way to the auroral E region, the fact that auroral field lines are nearly vertical means that the dispersion relations are applicable for only very short wavelengths, such that mapping (actually propagation!) of the polarization electric fields out of the E region can be ignored. For longer wavelengths, the polarization electric fields propagate along B and into the magnetosphere as Alfvén waves [Maltsev et al., 1977; Mallinckrodt and Carlson, 1978], which may be reflected and returned to the ionosphere, where they may feed back on the E region waves. In this work we derive a new branch of the ionospheric feedback instability that supports parallel electric fields and irregularities up to kilometer-scale in the E region. We argue that this dispersion relation is necessary to extend the study of auroral E region microphysics to longer wavelengths, where the upward propagation of polarization electric fields along magnetic field lines, and the reflections that return, cannot be ignored.

POLA-10 Correlation as a global measure of geomagnetic activity: Phase boundaries and a precedent line of nodes - by Russell Cosgrove

Status of First Author: Non-student

Authors: Russell Cosgrove and Ennio Sanchez

Abstract: This work considers the global correlation of geomagnetic activity as a way to evaluate magnetotail disturbances, such as the substorm. Impulsive magnetotail disturbances are generally associated with geomagnetic pulsations, which can be coherent over wide ranges of latitude and longitude, and which display distinctive phase reversals collocated with power maxima. Analyzing a disturbance period chosen for its breadth in local time, we find that pulsations can be detected from the coherence that they generate within a magnetometer array, and identify an extended line of nodes across which the phase reversals occur. Phase reversals consistent with the same line of nodes persist for five hours, beginning clearly in a 0.7 mHz pulsation one and a half hours before the disturbance, and persisting in a 5.8 mHz pulsation three and one half hours after the initial disturbance. Under the hypothesis that the line of nodes maps to a source in the central plasma sheet (CPS), we note that the persistence of this extended source of disturbances suggests memory in the CPS. We define a quantitative “coherence index” that characterizes geomagnetic activity according to the degree of global coherence that it generates, and observe that a narrowly peaked coherence signal leads a much broader peak in power. We relate these results to models of the magnetosphere based in critical phenomena.

POLA-11 CHAMP Estimates of Fluctuating Small-Scale Field-Aligned Currents and Their Relation to Flickering Aurora - by Rasoul Kabirzadeh

Status of First Author: Student IN poster competition

Authors: Rasoul Kabirzadeh

Abstract: We present CHAMP observations of intense transverse magnetic field fluctuations (10-20 nT amplitude) at frequencies of 1-15 Hz as the satellite crosses visible auroral arcs seen by the THEMIS ground-based camera array. Fluctuations in this frequency range are caused by small-scale FACs and they are consistent with published observations of auroral flicker observed both by ground-based cameras and in-situ. While the THEMIS cameras are not able to resolve the flicker itself, they allow us to associate the magnetic oscillations observed in-situ with strong, northward expanding, multiple auroral arcs. In two cases, the oscillations occur within quasi-static upward FAC channels tens of km wide and with amplitudes of 2-5 μ A/m². In a third example, the magnetic fluctuations detected by CHAMP show no low-frequency component, indicating no quasi-static (“DC”) upward FAC associated with the arc. In fact CHAMP detects a strong downward current within or near the arc, suggesting that all of the visible emission observed by the cameras is due entirely to oscillating fields with no static component. An additional new aspect of these magnetic observations is the presence of strong harmonics at multiples of the ~3 Hz fundamental oscillation.

POLA-12 A Proposed Spatial Heterodyne Spectrometer for Measurement of the Proton Aurora at High Latitude - by Steven Watchorn

Status of First Author: Non-student, PhD

Authors: S. Watchorn

Abstract: A new Spatial Heterodyne Spectrometer (SHS) is proposed to measure emissions from the proton aurora at high latitudes (near the edge of the auroral oval). This work follows observations made from Tromsø, Norway, using the High Throughout Imaging Echelle Spectrograph (HiTIES). That instrument observed four distinct spectral regions (H-alpha and -beta, N₂⁺ 1 NG at 427 nm, and redline oxygen emissions at 630 nm) to determine the dynamics of the proton aurora on short (4 minute) time

scales. The latter two emissions in the list above provided information about electron emissions during the observation period.

The prospective SHS will be able to duplicate the spectral coverage of HiTIES with the Jacquinot advantage inherent to an interferometer compared to a slit spectrometer. Simple rotation of the SHS gratings (and assured relatively constant efficiency over the wavelength span of interest) will allow the SHS to sample different emissions in turn. Alternatively, multiple tabletop SHS's could provide the spectral coverage at the resolution necessary to follow the work of HiTIES.

POLA-13 Altitudinal distribution of Joule heating and its influence on the thermosphere - by Yanshi Huang

Status of First Author: Student IN poster competition

Authors: Yanshi Huang, Arthur Richmond, Yue Deng, Ray Roble

Abstract: Studies of the thermospheric response to Joule heating cannot consider only the height-integrated heating, as approximated by the downward Poynting flux above the ionosphere, but must also consider how this heat is distributed in altitude. The National Center for Atmospheric Research Thermosphere-Ionosphere-Electrodynamics General Circulation Model (NCAR TIE-GCM) is employed to quantify the influence of Joule heating at different altitudes on the neutral temperature and density at 400km for both solar minimum and maximum conditions. The results show that high-altitude Joule heating is more efficient than low-altitude heating in affecting the upper thermosphere. Most of the Joule heating is deposited under 150km, and the largest Joule heating deposition per scale height happens at about 125km, independent of solar activity. However, the temperature and density changes at 400km are largest for heat deposited at about 140km for solar minimum and about 263km for solar maximum. The time scale for the thermospheric response varies with the altitude of heating. Joule heating deposited at lower heights needs more time to conduct upward, and it takes more time for the thermosphere at 400km to approach a steady state. A simple one-dimensional model is utilized to explain how the amplitude and characteristic time scale of the upper thermosphere response to Joule heating depends on the height of heat input. The characteristic response time scale for heat deposited around 135km is 6 hours, while that for heat deposited around 238km is about 0.5 hours. The initial temperature response at 400km to the high-altitude heating is much stronger than the response to the low-altitude heating, but the responses become comparable after about 4 days.

POLA-14 Altitude and latitude variation of Thermosphere Mass Density Response to Geomagnetic Activity in Composition Transition Regions - by Xianjing Liu

Status of First Author: Student NOT poster competition, PhD

Authors: X. Liu¹, J. P. Thayer¹, A. Burns², W. Wang² and J. Lei³

¹University of Colorado, Aerospace Engineering Sciences Department, Boulder CO

²National Center for Atmospheric Research, Boulder CO

³Univ. of Sci. & Tech. of China, School of Earth and Space Sciences, Hefei, Anhui, China

Abstract: The thermosphere mass density response with altitude and latitude to solar wind high-speed streams is investigated using the mass density observation data inferred from accelerometer measurements on the CHAMP and GRACE satellites during the recent solar minimum. The predominance of helium suppressed the density response in the winter hemisphere near the GRACE altitude during this solar minimum. The general concept of scale height and the MSIS model are employed to separate the mean molecular weight effect from the temperature effect on mass density response with altitude and latitude. The MSIS simulation indicates that, in regions of composition transition, the composition effect on the mass density response can be larger than the temperature effect. The vertical gradient of the logarithmic mean molecular weight peaks at both nitrogen/oxygen and oxygen/helium transition regions and decreases the mass density scale height. The composition affect at the oxygen/helium transition is greater than at the

nitrogen/oxygen transition and can decrease the mass density scale height by more than 40% in this solar minimum playing an important role in the total mass density response to geomagnetic activity.

**POLA-15 Vertical Winds in the Southern Auroral Thermosphere Observed
Concurrently at E- and F-region Altitudes - by Callum Anderson**

Status of First Author: Non-student

Authors: C. Anderson, M. Conde, T. Davies, P. Dyson, M. J. Kosch

Abstract: Vertical winds are a poorly understood component of the upper atmospheric circulation. Vertical hydrostatic stability, coupled with the strong positive temperature gradient that exists throughout the region, should effectively damp the motion of air parcels normal to constant pressure surfaces. However, observations of fast (50-100 m/s) vertical winds have been reported in the literature. As a consequence of the difficulties associated with observing vertical atmospheric motions at these altitudes, we also have very little knowledge of the horizontal spatial structure of the vertical wind field, and even less of the vertical structure.

During 2011, a campaign of bistatic observations was conducted using two Fabry-Perot spectrometers in Antarctica. Both instruments were configured to interleave their observations between E- and F-region altitudes. By combining the data from both instruments, estimates were made of the E-region vertical wind at 4 locations, and the F-region vertical wind at 5 locations, spanning a magnetic latitude range of approximately 4°. Here we present results from that campaign, and demonstrate both the horizontal and vertical structure that was observed.

**POLA-16 Coincidental measurements of an F-region plasma patch, with optical,
incoherent and coherent scatter radar instruments
- by Gareth William Perry**

Status of First Author: Student IN poster competition, PhD

Authors: G. W. Perry (1)

H. Dahlgren (2)

J.-P. St.-Maurice (1)

J. L. Semeter (2)

K. Hosokawa (3)

M. J. Nicolls (4)

M. Greffen (5),

K. Shiokawa (6)

C. Heinselman (4)

(1) Institute for Space and Atmospheric Studies, Department of Physics and Engineering Physics, University of Saskatchewan, Canada.

(2) The Department of Electrical and Computer Engineering, Boston University, USA.

(3) Department of Communication Engineering and Informatics, University of Electro-Communications, Japan.

(4) SRI International, USA.

(5) University of Calgary, Canada.

(6) Solar-Terrestrial Environment Laboratory, Nagoya University, Japan.

Abstract: The spatial and temporal evolution of an F-region plasma patch, detected over Resolute Bay, has been studied with a suite of instruments. For this case study, the Resolute Incoherent Scatter Radar - North (RISR-N) is used to construct a three-dimensional image of the patch. Multiple Super Dual Auroral Radar Network (SuperDARN) systems along with the Optical Mesosphere Thermosphere Imagers (OMTI) and Narrow-band All-Sky Camera for Auroral Monitoring (NASCAM) imagers at Resolute Bay are used to provide a multi-instrument overview of the high latitude F region during the event. SuperDARN was used

to track the patch for nearly an hour, from the cusp region to Resolute Bay. During a 10 minute period, the patch was detected and identified in the RISR-N, OMTI and SuperDARN instruments, yielding a unique opportunity to study the patch with multiple instruments. Of the more interesting findings of this study, evidence of significant density fluctuations within the patch is detected without any clear indication of an external driver such as precipitation.

POLA-17 Infrasonic waves generated by supersonic auroral arcs - by Victor Pasko

Status of First Author: Non-student

Authors: Victor P. Pasko, CSSL, Penn State University, University Park, Pennsylvania, USA
(vpasko@psu.edu)

Abstract: A finite-difference time-domain (FDTD) model of infrasound propagation in a realistic atmosphere is used to provide quantitative interpretation of infrasonic waves produced by auroral arcs moving with supersonic speed. In the FDTD model, the altitude and frequency dependent attenuation coefficients provided by Sutherland and Bass [J. Acoust. Soc. Am., 115, 1012, 2004] are included in classical equations of acoustics in a gravitationally stratified atmosphere using a decomposition technique recently proposed by de Groot-Hedlin [J. Acoust. Soc. Am., 124, 1430, 2008] and employed in [de Larquier et al., GRL, 37, L06804, 2010; de Larquier, MS Thesis, Penn State, Aug. 2010].

The auroral infrasonic waves (AIW) in the frequency range 0.1-0.01 Hz associated with the supersonic motion of auroral arcs have been extensively studied for over four decades [e.g., Wilson, Inframatics, (10), 1, 2005, and references therein], and the Lorentz force and Joule heating are discussed in the existing literature as primary sources producing infrasound waves associated with auroral electrojet. Our quantitative numerical results are consistent with original ideas of Swift [JGR, 78, 8205, 1973] and demonstrate that the synchronization of the speed of auroral arc and phase speed of the acoustic wave in the electrojet volume is an important condition for generation of magnitudes and frequency contents of infrasonic waves observable on the ground. It is shown in [Swift, 1973] that unless the subsonic electrojet is moving at speeds very close to the speed of sound, the frequency components generated would be so low that the wave would be unobservable. Supersonic electrojets generate enough high-frequency components to be observable over a wide range of speeds, but with diminishing amplitude as the speed increases above the sonic speed [Swift, 1973].

POLA-18 Direct observations of the role of convection electric fields in the formation of a polar tongue of ionization from storm enhanced density - by Evan Thomas

Status of First Author: Student IN poster competition, Masters

Authors: E. G. Thomas (1), J. B. H. Baker (1), J. M. Ruohoniemi (1), S. G. Shepherd (2), E. R. Talaat (3), A. J. Coster (4), J. C. Foster (4), P. J. Erickson (4)
(1) Virginia Tech, (2) Dartmouth College, (3) The Johns Hopkins University Applied Physics Laboratory, (4) MIT Haystack Observatory

Abstract: A tongue of ionization (TOI) is a channel of high-density F region plasma transported from the dayside mid-latitude ionosphere through the cusp and into the polar cap by enhanced convection electric fields. Previously, mid-latitude plumes of ionization, known as storm enhanced density (SED), carried sunward and poleward by the low-latitude edge of the sub-auroral polarization stream have been suggested as the dayside source of polar TOI. However, SED plumes have also been observed over North America without any evidence of the formation of a TOI. To better understand the mechanisms which cause the formation of a polar TOI from an SED plume, we present simultaneous total electron content (TEC) observations from ground-based GPS receivers and ionospheric backscatter recorded by SuperDARN radars during a geomagnetic storm on 26-27 September 2011. The recent expansion of the SuperDARN network to mid-latitudes allows for detailed comparison between convection electric fields and the motion

of large-scale TEC features seen in the region of high density GPS measurements. This storm can be separated into two periods of interest: (1) an hour-long period of dynamic geomagnetic activity from 18:30-19:30 UT on 26 September 2011 during which a channel of high-density F region plasma is transported through the dayside cusp and across the polar cap at velocities in excess of 1400 m/s by enhanced convection electric fields extending to middle latitudes, and (2) a later period of quiet geomagnetic activity during which a high-TEC feature persists for several hours as it co-rotates with the Earth but does not get entrained in the poleward flows. These results suggest that an SED plume can be classified as either actively being driven sunward and poleward to form a TOI, or as an inactive “fossil SED” co-rotating with the Earth at a near constant latitude. In this talk we will analyze these first-ever direct observations of the role of convection electric fields at mid-latitudes in structuring ionospheric plasma from the mid-latitudes to the polar cap.

Solar Terrestrial Interactions in the Upper Atmosphere

SOLA-01 Improving CTIPe neutral density response and recovery during large geomagnetic storms - by Mariangel Fedrizzi

Status of First Author: Non-student, PhD

Authors: M. Fedrizzi, T. Fuller-Rowell, M. Codrescu, M. G. Mlynczak, D. R. Marsh

Abstract: The temperature of the Earth’s thermosphere can be substantially increased during geomagnetic storms mainly due to high-latitude Joule heating induced by magnetospheric convection and auroral particle precipitation. Thermospheric heating increases atmospheric density and the drag on low-Earth orbiting satellites. The main cooling mechanism controlling the recovery of neutral temperature and density following geomagnetic activity is infrared emission from nitric oxide (NO) at 5.3 micrometers. NO is produced by both solar and auroral activity, the first due to solar EUV and X-rays the second due to dissociation of N₂ by particle precipitation, and has a typical lifetime of 12 to 24 hours in the mid and lower thermosphere. NO cooling in the thermosphere peaks between 150 and 200 km altitude. In this study, a global, three-dimensional, time-dependent, non-linear coupled model of the thermosphere, ionosphere, plasmasphere, and electrodynamics (CTIPe) is used to simulate the response and recovery timescales of the upper atmosphere following intense geomagnetic activity. CTIPe uses time-dependent estimates of NO obtained from Marsh et al. [2004] empirical model based on Student Nitric Oxide Explorer (SNOE) satellite data rather than solving for minor species photochemistry self-consistently. This empirical model is based solely on SNOE observations, when K_p rarely exceeded 5. During conditions between K_p 5 and 9, a linear extrapolation has been used. In order to improve the accuracy of the extrapolation algorithm, CTIPe model estimates of global NO cooling have been compared with the NASA TIMED/SABER satellite measurements of radiative power at 5.3 micrometers. The comparisons have enabled improvement in the timescale for neutral density response and recovery during extreme conditions of geomagnetic storms. CTIPe neutral density response and recovery rates are verified by comparison CHAMP satellite observations.

SOLA-02 On the Validation effort of the Coupled Thermosphere Ionosphere Plasmasphere electrodynamics Model - by Catalin Negrea

Status of First Author: Student IN poster competition, PhD

Authors: C. Negrea, M. V. Codrescu, T. J. Fuller-Rowell

Abstract: The Coupled Thermosphere Ionosphere Plasmasphere electrodynamics model (CTIPe) has proven to be a valuable ionospheric research tool. Improving our knowledge of systematic and seasonal model biases is necessary if further improvements are to be made. This paper presents the next step in our verification and validation effort and in developing a standardized analysis methodology. A semi-automated software part of the near-real-time-run of CTIPe is described and results derived from its usage are presented. Model limitations and biases are detailed for the electron density profile peak (NmF₂) and its

corresponding height (hmF2). Model performance for hmF2 is constant throughout the whole year, with an average 10% deviation from observed values. There is a strong seasonal variation for NmF2, with greater deviations from the observed trends during summer. This effect seems to have latitude dependence, although the gaps in the available data do not allow for an exact determination of its nature.

SOLA-03 Intense dayside Joule heating during the 5 April 2010 geomagnetic storm recovery phase observed by AMIE and AMPERE - by Frederick Wilder

Status of First Author: Non-student, PhD

Authors: F. D. Wilder, G. Crowley, B. J. Anderson and A.D. Richmond

Abstract: When the interplanetary magnetic field (IMF) is northward, dawnward, or duskward, magnetic merging between the IMF and the geomagnetic field occurs near the cusp of the magnetosphere. While these periods are usually considered “quiet,” they can lead to intense, but highly localized, energy deposition into the dayside ionosphere. We identify such an occurrence during a series of two geomagnetic storms on 5 April 2010. Using data from the Active Magnetosphere and Planetary Electrodynamics Response Experiment (AMPERE) for the first time as an input to the Assimilative Mapping of Ionospheric Electrodynamics (AMIE) algorithm, we show that during the recovery phase of the first storm there is intense ionospheric Joule heating in the dayside polar regions. This is associated with an intense field-aligned current pair near the noon meridian that is associated with northward IMF and a strong IMF By component. AMIE outputs are used to drive the thermosphere-ionosphere-mesosphere electrodynamics general circulation model to demonstrate that the intense levels of Joule heating can lead to anomalous thermospheric density enhancements and traveling disturbances.

SOLA-04 The Thermosphere and Ionosphere Reactions to the 15 February 2011 Solar Flare - by Jie Zhu

Status of First Author: Student IN poster competition, PhD

Authors: J. Zhu and A. J. Ridley, Department of Atmospheric, Oceanic and Space Sciences, University of Michigan, Ann Arbor

Abstract: Solar flares impact the thermosphere and ionosphere with sudden energy input of soft X-ray and solar extreme ultraviolet radiance. The reaction of the upper atmosphere to solar flares can be effected by other external forces. In this study, we run the Global Ionosphere-Thermosphere Model (GITM) during the 15 February 2011 solar flare to investigate how the reaction is influenced by the geometry of the Earth’s magnetic field, the high latitude driving by the interplanetary magnetic field (IMF) and the equatorial electrojet. The simulation that utilizes solar extreme ultraviolet flux from the Flare Irradiance Spectral Model (FISM) with all other external forcing constant except the irradiance is taken as a baseline. We then add each of the processes onto the baseline, in order to better understand how they work in conjunction with the solar flare to make a difference in the reaction. This study mainly focuses on the behavior of the neutral density and wind pattern of the thermosphere, as well as the perturbation of the total electron content (TEC) of the ionosphere. We also explore the coupling between the thermosphere and the ionosphere in response to the solar flare with each of the external processes included.

SOLA-05 Ionosphere/Thermosphere Model Assessment during the 2006 AGU Storm: TEC, NmF2 and hmF2 - by Ja Soon Shim

Status of First Author: Non-student

Authors: J. S. Shim*, M. Kuznetsova, L. Rastätter, D. Bilitza, M. Butala, M. Codrescu, B. A. Emery, B. Foster, T. J. Fuller-Rowell, J. Huba, A. J. Mannucci, X. Pi, A. Ridley, L. Scherliess, R. W. Schunk, J. J. Sojka, P. Stephens, and L. Zhu

Abstract: We evaluate Ionosphere/Thermosphere model performance during the 2006 AGU storm period. For this study, the selected physical parameters are Total Electron Content (TEC) obtained by GPS ground stations, and NmF2 and hmF2 from COSMIC LEO satellites. Models used for this study include empirical, physics based and data assimilation models. Modeled values are compared with global observations in the selected 5 degree eight longitude sectors. To quantify the performance of the models, skill scores are calculated using four different metrics. Furthermore, the skill scores are obtained for three latitude regions (low, middle and high latitudes) in order to investigate latitudinal dependence of the models' performance. This model validation study is supported by the Community Coordinated Modeling Center (CCMC) at the Goddard Space Flight Center. Model outputs and observational data used for the challenge will be permanently posted at the CCMC website (<http://ccmc.gsfc.nasa.gov>) as a resource for the space science communities to use.

SOLA-06 Climatology Assessment of Ionosphere/Thermosphere Models in Low Solar Flux Conditions for the CCMC CEDAR Challenge - by Barbara Emery

Status of First Author: Non-student

Authors: BA Emery (emery@ucar.edu, HAO/NCAR), JS Shim (CCMC/U MD), D Anderson (NOAA/U CO), D Bilitza (GSFC), J Chau (Jicamarca Radio Observatory Peru), G Crowley (ASTRA), M Codrescu (NOAA/SWPC), AJ Coster (MIT), JT Emmert (NRL), M Fedrizzi (NOAA/U CO), B Foster (HAO/NCAR), TJ Fuller-Rowell (NOAA/SWPC), LP Goncharenko (MIT), J Huba (NRL), L Lomidze (USU), H Lühr (GFZ Germany), AJ Mannucci (JPL), S McDonald (NRL), X Pi (JPL), A Ridley (U MI), L Scherliess (USU), R Schunk (USU), J Sojka (USU), DC Thompson (AFRL), E Sutton (AFRL), D Weimer (VT), and Q Wu (HAO/NCAR)

Abstract: The performance of Ionosphere/Thermosphere (IT) models during the solar minimum period from November 2007 to January 2008 (07325-08020) is evaluated for climatology. The climatology period was also separated into high-speed stream (HSS) and moderate Kp (≥ 2) and low-speed and low Kp (≤ 1) conditions where climatological days are found using median values of observations and model outputs to reflect the quiet solar minimum conditions. The physical parameters selected are: median values of the electron peak density and the height of this peak from COSMIC LEO satellites; median total electron content (TEC) from GPS satellites around 20,000 km observed at many ground stations from MIT and various labs contributing to IGS; two versions of neutral densities from the CHAMP satellite at 400 km and the satellite altitude (~350km) as well as ascending and descending node averages; global mean daily neutral densities from satellite drag analyses; and observed and estimated ion drifts at Jicamarca, Peru. Most of the IT models have been run at the Community Coordinated Modeling Center (CCMC) at the Goddard Space Flight Center (GSFC) using appropriate geophysical inputs for the CEDAR (Coupling, Energetics and Dynamics of Atmospheric Regions) ETI (Electrodynamics-Thermosphere-Ionosphere) Challenges. Other models include double resolution TIEGCM model runs using TIMED satellite SABER and TIDI temperature and wind lower boundary conditions, TIME-GCM/AMIE runs, SAMI3/HWM07/revised_MSIS00, and GITM. We examine 5 degree geographic latitude and 5-25 degree geographic longitude bins located in 8 longitude swaths with good ground TEC coverage. Data differences are examined to gain a good perspective on data errors and uncertainties. Percent deviations of model values from data are evaluated along with other metrics to better understand the strengths and weaknesses of various empirical, first principles, or assimilation ionosphere or coupled IT models.

SOLA-07 Height-Integrated Pedersen Conductivity of Ionosphere from COSMIC Observations - by Cheng Sheng

Status of First Author: Student IN poster competition

Authors: Cheng Sheng, Yue Deng, Yanshi Huang

Abstract: Altitude distribution of Joule heating is very important to the thermosphere and Ionosphere, which is proportional to the Pedersen conductivity at high latitudes. Using the COSMIC observations from

2008 to 2011, the height-integrated Pedersen conductivities in both E and F regions during the winter nighttime have been studied. Our result shows the ratio between the F and E region integrated Pedersen conductivities is about 1:4, which is larger than the ratio(1:10) generally expected in the auroral region. This indicates the energy input into the F region may be underestimated in empirical models. Since the electron density profile in E region from the COSMIC measurements may not be accurate, the comparison of conductivity between the COSMIC observations and empirical models has also been conducted. The variations of the ratio under different geomagnetic activities have been investigated as well.

Abarca, Accel, 11
Akbari, Hassanali, 13
Alonso, Ricardo, 16
Andersen, Carl, 18
Anderson, Callum, 34
Aveiro, Henrique, 4
Azeem, Irfan, 17

Bhattacharya, Tapas, 28

Chang, Fu-Yuan, 27
Chang, Loren, 22
Chen, Chao-Yen, 1
Cnossen, Ingrid, 23
Condor Patilongo, Percy, 20
Cosgrove, Russell, 31, 32
Cousins, Ellen, 30
Crowley, Geoff, 18

Dahlgren, Hanna, 30
Dao, Eugene, 10
Davidson, Ryan, 7
de Larquier, Sebastien, 12
Deshpande, Kshitija, 10
Despain, Kate, 12
Dodger, Aron, 24
Douglas, Ewan, 18
Duly, Timothy, 26

Edwin, Stanley, 29
Emery, Barbara, 38

Fedrizzi, Mariangel, 36
Fisher, Daniel, 4
Fu, Haiyang, 8
Fukushima, Daisuke, 3

Gehrels, Thomas, 16

Hackett, Alexander, 22
Hairston, Marc, 5
Hickey, Dustin, 25
Hirsch, Michael, 17
Huang, Yanshi, 33

Jafari, Ramin, 21
Jones, McArthur, 1

Kabirzadeh, Rasoul, 32
Kang-Hung, Wu, 7
Kiene, Andrew, 5
Kim, Hyomin, 10

Lee, I-Te, 15
Lee, Woo Kyoung, 6
Lin, Chi-Yen, 19
Lin, Jia-Ting, 25
Lin, Ting-han, 12
Lin, Yen-Chieh, 25
Liu, Xianjing, 33
Lomidze, Levan, 26

Madsen, Chad, 9
Mahmoudian, Alireza, 13
Mangogna, Tony, 18
Martinis, Carlos, 4
Mehta, Dhvanit, 5
Mei, Liyuan, 20
Miceli, Robert, 28
Milla, Marco, 21
Mills, Amanda, 14

Negrea, Catalin, 36
Nicolls, Michael, 14
Nooner, Jonathon, 24
Nossa, Eliana, 27
Nossal, Susan, 23

Pasko, Victor, 35
Perry, Gareth, 34

Reyes, Pablo, 11
Ribeiro, Alvaro, 11
Rodrigues, Fabiano, 15

Samimi, Alireza, 9
Sanders, Samuel, 27
Sarkhel, Sumanta, 2
Sheng, Cheng, 38
Shim, Ja Soon, 37

Shume, Esayas, 8
Sorbello, Robert, 3
Sousa, Austin, 14
Sun, Yang-Yi, 24

Thomas, Evan, 35
Tracy, Brian, 6

Urco, Juan, 22

Varney, Roger, 6

Warner, Kristi, 2
Watchorn, Steven, 32
Wendell , Horton, 9
Wilder, Frederick, 37
Wu, Qian, 29

Yamazaki, Yosuke, 1

Zablowski, Paul, 7
Zhu, Jie, 37